UNIVERSIDADE FEDERAL DO CEARÁ

CENTRO DE CIÊNCIAS

DEPARTAMENTO DE FÍSICO-QUÍMICA E QUÍMICA ANALÍTICA

PROGRAMA DE PÓS-GRADUAÇÃO EM QUÍMICA

LUCAS LIMA BEZERRA

ELECTROCHEMICAL AND THEORETICAL INVESTIGATION ON THE BEHAVIOR OF THE Co^{2+} ION IN THREE EUTECTIC SOLVENTS

FORTALEZA

2021

LUCAS LIMA BEZERRA

ELECTROCHEMICAL AND THEORETICAL INVESTIGATION ON THE BEHAVIOR OF THE Co^{2+} ION IN THREE EUTECTIC SOLVENTS

Dissertação apresentada ao Programa de Pós-Graduação em Química da Universidade Federal do Ceará como requisito parcial à obtenção do título de Mestre em Química. Área de concentração: Físico-Química.

Orientador: Profº. Dr. Norberto de Kássio Vieira Monteiro.

FORTALEZA

2021

Dados Internacionais de Catalogação na Publicação
Universidade Federal do Ceará
Biblioteca Universitária
Gerada automaticamente pelo módulo Catalog, mediante os dados fornecidos pelo(a) autor(a)

B469e Bezerra, Lucas Lima.
Electrochemical and theoretical investigation on the behavior of the Co2+ ion in three eutectic solvents / Lucas Lima Bezerra. – 2021.
68 f. : il. color.

Dissertação (mestrado) – Universidade Federal do Ceará, Centro de Ciências, Programa de Pós-Graduação em Química, Fortaleza, 2021.
Orientação: Prof. Dr. Norberto de Kássio Vieira Monteiro.

1. Deep eutectic solvents. 2. Cobalt. 3. Electrochemical techniques. 4. Computational simulations. I. Título.

CDD 540

LUCAS LIMA BEZERRA

ELECTROCHEMICAL AND THEORETICAL INVESTIGATION ON THE BEHAVIOR OF THE Co^{2+} ION IN THREE EUTECTIC SOLVENTS

Dissertação apresentada ao Programa de Pós-Graduação em Química da Universidade Federal do Ceará como requisito parcial à obtenção do título de Mestre em Química. Área de concentração: Físico-Química.

Aprovado em: __ / __ / ___.

BANCA EXAMINADORA

_____

Prof. Dr. Norberto de Kássio Vieira Monteiro (Orientador)

Universidade Federal do Ceará (UFC)

_____

Prof. Dr. Pedro de Lima Neto

Universidade Federal do Ceará (UFC)

_____

Prof. Dr. Emmanuel Silva Marinho

Universidade Estadual do Ceará (UECE)

To God.

To my parents, friends, and family.

ACKNOWLEDGMENTS

First, I thank God for my life, health and for giving me the ability to realize this dream!

To my father, mom, and sister, by all dedication and support independent of my dream. When I thought about in quit, none of them let that happen. Therefore, I always take with me this phrase: Quit did not become part of our vocabulary.

To all my friends: Francisco Wagner, Leonardo Paes, Demontier Mesquita, Emmanuele Machado, Conceição Regina, Pabllo Abreu, Reginaldo Júnior, Lucas Coutinho, Ámison Rick, Renato Verissímo, and Davi Cardoso for the friendship, advices and for all the legendary tours in Fortaleza.

To all members of GQT (Group of Chemistry Theoretical) for helping me develop the work of direct and indirect ways.

To professor Dr. João Bezerra Neto Rufino for teaching me the Gromacs *software* and for being available to clear up my doubts over the two years of the master's.

To professors Dr. Emmanuel Silva Marinho and Dr. Pedro de Lima Neto, you have opened the doors of your respective laboratories for me and by all contributions to this work.

To contribute realized by professor Dra. Adriana Nunes Correia and professor Dr. Pierre Basílio Almeida Fechine, thanks to you, I could improve this work more.

To professor Dr. Norberto de Kássio Vieira Monteiro, by trust, advice, and guide in constructing this work and by the availability of always sharing knowledge.

This study was financed in part by the Coordenação de Aperfeiçoamento de Pessoal de Nível Superior – Brasil (CAPES) – Finance Code 001.

‘‘Do not let people make you give up what you want most in life. Believe it. Fight. Conquer. Furthermore, above all, be happy.’’

(Unknown author)

ABSTRACT

Deep eutectic solvents have many advantages, making them a promising alternative in replacing ionic liquids and organic solvents. Besides, DESs has received much prominence due to its diverse applications: Electrodeposition of metals, organic synthesis, gas adsorption, and biodiesel production. Therefore, this work analyzed the effect of the temperature increase (298 K to 353 K) on the behavior of the Co^{2+} ions in three eutectic solvents through electrochemical techniques and computational simulations. From the electrochemical analysis carried out, the increase in temperature caused a reduction in specific mass and an increase in the diffusion coefficient. Besides, the activation energy values were of 15.3, 29.9, and 55.2 kJ mol^{-1} for 1ChCl:2EG, 1ChCl:2U, and 1ChCl:2G, respectively. The computational simulations indicate that the increased temperature effect caused the replacement of DLH molecules by anions chloride around Co^{2+} ions for the SDW1 and SDW3 systems between the temperatures of 298 K to 353 K, except for the SDW2 system that the replaced occurred in the interval of 313 K to 353 K. Besides, the increase of temperature occasioned the increase of strength for Co-Cl interaction and weakened the interactions between the Co^{2+} ions with the oxygen of DLH molecules.

Keywords: deep eutectic solvents; cobalt; electrochemical techniques; computational simulations.

RESUMO

Solventes eutéticos profundos possuem várias vantagens, tornando uma alternativa promissora para a substituição dos líquidos iônicos e solventes orgânicos. Além disso, esses solventes tem recebido muito destaque devido as suas diversas aplicações: eletrodeposição de metais, síntese orgânica, adsorção de gases e produção de biodiesel. Portanto, esse trabalho analisou o efeito do aumento da temperatura (298 K a 353 K) no comportamento dos íons Co^{2+} em três solventes eutéticos através de técnicas eletroquímicas e simulações computacionais. A partir da análise eletroquímica realizada, o aumento da temperatura ocasionou na redução da massa específica e um aumento no coeficiente de difusão. Além disso, os valores da energia de ativação foram de 15.3, 29.9 e 55.2 kJ mol^{-1} para 1ChCl:2EG, 1ChCl:2U e 1ChCl:2G, respectivamente. As simulações computacionais indicam que o aumento da temperatura ocasionou a substituição das moléculas de DLH por ânions cloreto em torno dos íons Co^{2+} para os sistemas SDW1 e SDW3 entre as temperaturas de 298 K e 353 K, exceto para o sistema SDW2 que a substituição ocorreu no intervalo de 313 K a 353 K. Além disso, o aumento da temperatura ocasionou o aumento na força da interação Co-Cl e enfraqueceu as interações entre os íons Co^{2+} com os oxigênios das moléculas de DLH.

Palavras-chave: solvente eutético profundo; cobalto; técnicas eletroquímicas; simulações computacionais.

LIST OF FIGURES

Figure 1 - Structures used in the MD simulations and nomenclature of main atoms. (a) ethylene glycol, (b) urea, (c) glycerol, (d) choline, (e) cobalt, and (f) chloride.....24

Figure 2 - Cyclic voltammograms obtained on Cu electrode in (a) 1ChCl:2EG, (b) 1ChCl:2G, and (c) 1ChCl:2U containing 0.1 mol L^{-1} $CoCl_2.6H_2O$ at several temperatures. Scan rate of 10 mV s^{-1}.....26

Figure 3 - Arrhenius plots of diffusion coefficient of Co^{2+} species in (a) 1ChCl:2EG, (b) 1ChCl:2G, and (c) 1ChCl:2U……..…….....28

Figure 4 - Stokes-Einstein plots obtained from (a) 1ChCl:2EG, (b) 1ChCl:2G, and (c) 1ChCl:2U…….…….....29

Figure 5 - Correlation between the values of specific mass obtain though of experimental and theoretical methods in function of temperature. Systems simulated: (a) SDW1, (b) SDW2, and (c) SDW3…….……..30

Figure 6 - Correlation between the diffusion coefficient obtain though of experimental and theoretical methods in function of temperature. Systems simulated: (a) SDW1, (b) SDW2, and (c) SDW3……..30

Figure 7 - Radial distribution functions (RDF) of Co^{2+} ions with atoms present in the SDW1 system, at temperatures (a) 298 K, (b) 313 K, (c) 333 K, and (d) 353 K …… 32

Figure 8 - Cumulative number (CN) of (a) Co-Cl, (b) Co-(O1, O2), and (c) Co-Ow interactions …….33

Figure 9 - Spatial distribution function (SDF) between Co^{2+} ions with components present in the SDW1 system, at temperatures (a) 298 K and (b) 353 K. Co^{2+} (red); chloride (green, isovalue = 0.0013); ethylene glycol (blue, isovalue = 0.0105); water (yellow, isovalue = 0.0004)……34

Figure 10 - Molecular graphs with intramolecular interactions and BCP of the Co^{2+} ion with the SDW1 system, at temperatures of (a) 298 K and (b) 353 K …….36

Figure 11 - Radial distribution functions (RDF) of Co^{2+} ions with atoms present in the SDW2 system, at temperatures (a) 298 K, (b) 313 K, (c) 333 K, and (d) 353 K …… 37

Figure 12 - Cumulative number (CN) of (a) Co-Cl, (b) Co-O3, and (c) Co-Ow interactions ……38
Figure 13 - Spatial distribution function (SDF) between Co^{2+} ions with components present in the SDW2 system, at temperatures (a) 313 K and (b) 353 K. Co^{2+} (red); chloride (green, isovalue = 0.0038); urea (blue, isovalue = 0.0127); water (yellow, isovalue = 0.0007)……...39
Figure 14 - Molecular graphs with intramolecular interactions and BCP of the Co^{2+} ion with the SDW2 system, at temperatures of (a) 313 K and (b) 353 K …...…....41
Figure 15 - Radial distribution functions (RDF) of Co^{2+} with atoms present in the SDW3 system, at temperatures (a) 298 K, (b) 313 K, (c) 333 K, and (d) 353 K……...42
Figure 16 - Cumulative number (CN) of (a) Co-Cl, (b) Co-(O4,O5,O6), and (c) Co-Ow interactions ……43
Figure 17 - Spatial distribution function (SDF) between Co^{2+} ions with components present in the SDW3 system, at temperatures (a) 298 K and (b) 353 K. Co^{2+} (red); chloride (green, isovalue = 0.0047); glycerol (blue, isovalue = 0.0122); water (yellow, isovalue = 0.0027)……44
Figure 18 - Molecular graphs with intramolecular interactions and BCP of the Co^{2+} ion with the SDW3 system, at temperatures of (a) 298 K and (b) 353 K ……...46

LIST OF FIGURES – SUPPLEMENTARY MATERIAL

Figure S1 - The amount of water in DES in ppm as a function of the number of days under the ambient atmosphere. The results are an average of three measurements over a week.....53

Figure S2 - Cyclic voltammograms obtained for Cu electrode in (a) 1ChCl:2EG, (b) 1ChCl:2G, and (c) 1ChCl:2U blank electrolyte. Scan rate 10 mV s^{-1}.....53

Figure S3 - Current-time transients for the reduction of Co^{2+}/Co on Cu substrate obtained from DES 1ChCl:2EG (a) 298 K, (b) 313 K, (c) 333 K, and (d) 353 K containing 0.1 mol L^{-1} $CoCl_2.6H_2O$. Insets: Cottrell´s plots are showed as insert…….....54

Figure S4 - Current-time transients for the reduction of Co^{2+}/Co on Cu substrate obtained from DES 1ChCl:2G (a) 298 K, (b) 313 K, (c) 333 K, and (d) 353 K containing 0.1 mol L^{-1} $CoCl_2.6H_2O$. Insets: Cottrell´s plots are showed as insert……..... 54

Figure S5 - Current-time transients for the reduction of Co^{2+}/Co on Cu substrate obtained from DES 1ChCl:2U (a) 298 K, (b) 313 K, (c) 333 K, and (d) 353 K containing 0.1 mol L^{-1} $CoCl_2.6H_2O$. Insets: Cottrell´s plots are showed as insert……..... 55

LIST OF TABLES

Table 1 - Number of molecules and ions present in each system used in MD simulations..... 24

Table 2 - Topological data for Co^{2+} interactions with SDW1 system, at temperatures of 298 K and 353 K. Electron density, ρ(r), Laplacian of electron density, $\nabla^2\rho$(r), ELF value, η(r), at bond critical points (BCP) of selected Co-Cl and Co-(O1,O2) interactions.....35

Table 3 - Topological data for Co^{2+} interactions with SDW2 system, at temperatures of 313 K and 353 K. Electron density, ρ(r), Laplacian of electron density, $\nabla^2\rho$(r), ELF value, η(r), at bond critical points (BCP) of selected Co-Cl and Co-O3 interactions……... 40

Table 4 - Topological data for Co^{2+} interactions with SDW3 system, at temperatures of 298 K and 353 K. Electron density, ρ(r), Laplacian of electron density, $\nabla^2\rho$(r), ELF value, η(r), at bond critical points (BCP) of selected Co-Cl and Co-(O4,O5,O6) interactions……...……...……...45

LIST OF TABLES – SUPPLEMENTARY MATERIAL

Table S1 - Effect of temperature on the viscosity of 1ChCl:2EG, 1ChCl:2U, and 1ChCl:2G containing 0.1 mol L^{-1} $CoCl_2.6H_2O$.....51

Table S2 - The values of diffusion coefficients for Co^{2+} species calculated by the Cottrell method.....52

LIST OF ABBREVIATIONS AND ACRONYMS

BCP	Bond Critical Point
CN	Cumulative Number
CVs	Cyclic Voltammograms
DESs	Deep Eutectic Solvents
DFT	Density Functional Theory
EG	Ethylene Glycol
ELF	Electron Localization Function
G	Glycerol
HBA	Hydrogen Bond Acceptor
HBD	Hydrogen Bond Donor
ILs	Ionic Liquids
LANL2DZ	Los Alamos National Laboratory 2-double-z
MD	Molecular Dynamics
OPLS-AA	Optimized Potentials for Liquid Simulations – All Atom
QTAIM	Quantum Theory of Atoms in Molecules
RDF	Radial Distribution Function
RTILs	Room Temperature Ionic Liquids
SDF	Spatial Distribution Function
U	Urea

SUMMARY

1 INTRODUCTION.....16

2 ELECTROCHEMICAL AND THEORETICAL INVESTIGATION ON THE BEHAVIOR OF THE Co^{2+} ION IN THREE EUTECTIC SOLVENTS..... 18

3 CONCLUSION.....58

4 REFERENCES.....59

APPENDIX A – AUTOR'S CURRICULAR DATA.....61

APPENDIX B – PAPER PUBLISHED.....64

APPENDIX C – PAPER SUBMITTED 65

1 INTRODUCTION

The Deep eutectic solvents (DESs) are known as a new class of ionic liquid (ILs) analogs due to their similar physical properties, among them: Low vapor pressure, relatively wide liquid range, and nonflammability (SMITH; ABBOTT; RYDER, 2014). Besides, the DESs have several advantages concerning traditional ILs such as easy preparation, low cost (ZHANG *et al*., 2012), high purity, and biodegradable. DESs are usually obtained through the complexation of a quaternary ammonium salt with a metal salt or hydrogen donor bond (HBD) (SMITH; ABBOTT; RYDER, 2014). The main property observed in the DESs is the decrease of the melting point of the mixture concerning the isolated components pure.

The interest in DESs has been increasing in recent years due to the vantages cited above, consequently, this solvent has been applied in several areas, such as biodiesel production (ZHAO; BAKER, 2013), chemistry synthesis (SMITH; ABBOTT; RYDER, 2014), adsorption and capture CO_2 (GARCIA *et al*., 2015), polymers synthesis (CARRIAZO *et al*., 2012), enzyme catalysis (GORKE; SRIENC; KAZLAUSKAS, 2008), and electrochemical (SMITH; ABBOTT; RYDER, 2014).

The electrodeposition of metals and metal alloys is a main electrochemical field that has been employed the use of DESs due to the high solubility of metal salts, and the high conductivity. Besides, most DESs have a wide electrochemical window concerning the water. Therefore, the use DESs is favored in the electrodeposition of metals (BARRADO *et al*., 2018). Several articles were published utilized the DESs in the electrodeposition of Co-Cr (SARAVANAN; MOHAN, 2012), Sn (ABBOTT *et al*., 2007), In (ALCANFOR *et al*., 2017), Ni (ABBOTT *et al*., 2015), and Cu (ABBOTT *et al*., 2009; SEBASTIÁN; VALLÉS; GÓMEZ, 2014).

One of the most recent articles utilizing the DESs in the electrodeposition of metals was published by Bezerra-Neto *et al* (BEZERRA-NETO *et al*., 2020). This article analyzed the effect of water on the behavior of Ag^+ ions in DESs based on urea and choline chloride. According to Bezerra-Neto *et al* (BEZERRA-NETO *et al*., 2020), the increase in the percentual of water occasioned the replacement of a few urea molecules by water molecules around the Ag^+ ions. Besides, another article too published by Bezerra-Neto *et al* (BEZERRA-NETO *et al*., 2018) analyzed the effect of water on the behavior of Cu^{2+} ions in DESs based on ethylene glycol and chloride choline. The results indicated that the increase of percentual of water occasioned in replacing ethylene glycol molecules by water molecules around Cu^{2+} ions.

In both articles cited above were utilized two complementary approaches. The first approach was used electrochemical techniques through Cyclic Voltammetry (CVs) to obtain the operating electrochemical potential range in the DESs. The computational simulations by Molecular Dynamics (MD) were used as the second approach to understanding the behavior at the molecular level of Ag^{+} ions in the urea-chloride choline (BEZERRA-NETO *et al.*, 2020) and Cu^{2+} ions in ethylene glycol-chloride choline (BEZERRA-NETO *et al.*, 2018).

Until now, the electrodeposition of cobalt in the DESs was not analyzed together by both approaches cited above. Then, the cobalt metal was chosen due to the applications as electrocatalysis (XU, 2019), sensors (LI, 2019), biomedical applications (LIM; MAJETICH, 2013), and antibacterial activity (SYED KHADAR *et al.*, 2019). The master's dissertation presented is about the behavior of the Co^{2+} ion in three eutectic solvents through an electrochemical analysis by cyclic voltammetry and chronoamperometry techniques, followed by computational simulations by molecular dynamics and QTAIM calculations. All these systems were obtained and analyzed in the period from June 2019 to June 2021.

Chapter 1

ELECTROCHEMICAL AND THEORETICAL INVESTIGATION ON THE BEHAVIOR OF THE Co^{2+} ION IN THREE EUTECTIC SOLVENTS

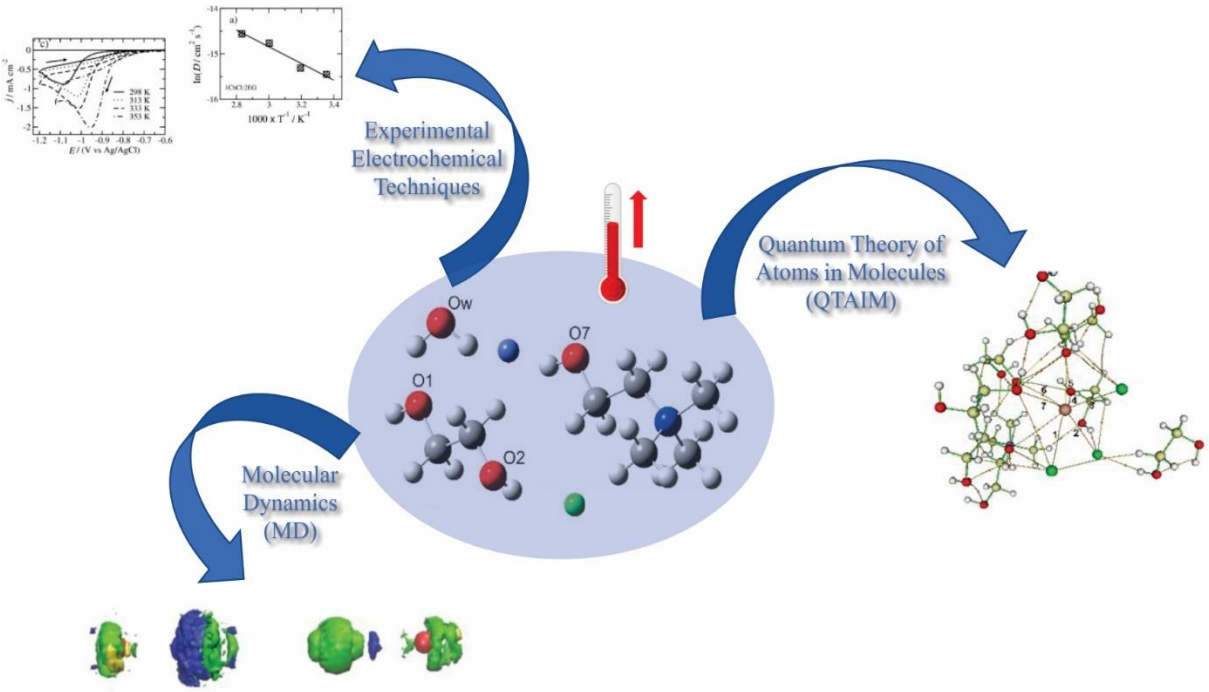

Experimental and computational approaches for analyzing the temperature effect on the behavior of the Co^{2+} ions in eutectic solvents.

Journal of Molecular Graphics and Modelling

Electrochemical and theoretical investigation on the behavior of the Co2+ ion in three eutectic solvents

--Manuscript Draft--

Manuscript Number:	JMGM-D-21-00978
Article Type:	Full Length Article
Keywords:	Deep eutectic solvents; Cobalt; Electrochemical techniques; Computational simulations
Corresponding Author:	Norberto Monteiro Universidade Federal do Ceara BRAZIL
First Author:	Lucas Lima Bezerra
Order of Authors:	Lucas Lima Bezerra
	Francisco Gilvane Sampaio Oliveira
	Luis Paulo Mourão dos Santos
	Hosiberto Batista de Sant'Ana
	Filipe Xavier Feitosa
	Adriana Nunes Correia
	Walther Schwarzacher
	Emmanuel Silva Marinho
	Pedro de Lima-Neto
	Norberto Monteiro
Abstract:	Deep eutectic solvents (DESs) have many advantages, making them a promising alternative in replacing ionic liquids and organic solvents. Besides, DESs has received much prominence due to its diverse applications: Electrodeposition of metals, organic synthesis, gas adsorption, and biodiesel production. Therefore, this work analyzed the effect of the temperature increase (298 K to 353 K) on the behavior of the Co^{2+} ions in three eutectic solvents through electrochemical techniques and computational simulations. From the electrochemical analysis carried out, the increase in temperature caused a reduction in specific mass and an increase in the diffusion coefficient. Besides, the activation energy values were of 15.3, 29.9, and 55.2 kJ mol^{-1} for 1ChCl:2EG, 1ChCl:2U, and 1ChCl:2G, respectively. The computational simulations indicate that the increased temperature effect caused the replacement of HBD molecules by anions chloride around Co^{2+} ions for the SDW1 and SDW3 systems between the temperatures of 298 K to 353 K, except for the SDW2 system that the replaced occurred in the interval of 313 K to 353 K. Besides, the increase of temperature occasioned the increase of strength for Co-Cl interaction and weakened the interactions between the Co^{2+} ions with the oxygen of HBD molecules.

RESUMO

Solventes eutéticos profundos possuem várias vantagens, tornando uma alternativa promissora para a substituição dos líquidos iônicos e solventes orgânicos. Além disso, esses solventes tem recebido muito destaque devido as suas diversas aplicações: eletrodeposição de metais, síntese orgânica, adsorção de gases e produção de biodiesel. Portanto, esse trabalho analisou o efeito do aumento da temperatura (298 K a 353 K) no comportamento dos íons Co^{2+} em três solventes eutéticos através de técnicas eletroquímicas e simulações computacionais. A partir da análise eletroquímica realizada, o aumento da temperatura ocasionou na redução da massa específica e um aumento no coeficiente de difusão. Além disso, os valores da energia de ativação foram de 15.3, 29.9 e 55.2 kJ mol^{-1} para 1ChCl:2EG, 1ChCl:2U e 1ChCl:2G, respectivamente. As simulações computacionais indicam que o aumento da temperatura ocasionou a substituição das moléculas de DLH por ânions cloreto em torno dos íons Co^{2+} para os sistemas SDW1 e SDW3 entre as temperaturas de 298 K e 353 K, exceto para o sistema SDW2 que a substituição ocorreu no intervalo de 313 K a 353 K. Além disso, o aumento da temperatura ocasionou o aumento na força da interação Co-Cl e enfraqueceu as interações entre os íons Co^{2+} com os oxigênios das moléculas de DLH.

Palavra-chave: Solvente eutético profundo; Cobalto; Técnicas eletroquímicas; Simulações computacionais.

ABSTRACT

Deep eutectic solvents (DESs) have many advantages, making them a promising alternative in replacing ionic liquids and organic solvents. Besides, DESs has received much prominence due to its diverse applications: Electrodeposition of metals, organic synthesis, gas adsorption, and biodiesel production. Therefore, this work analyzed the effect of the temperature increase (298 K to 353 K) on the behavior of the Co^{2+} ions in three eutectic solvents through electrochemical techniques and computational simulations. From the electrochemical analysis carried out, the increase in temperature caused a reduction in specific mass and an increase in the diffusion coefficient. Besides, the activation energy values were of 15.3, 29.9, and 55.2 kJ mol^{-1} for 1ChCl:2EG, 1ChCl:2U, and 1ChCl:2G, respectively. The computational simulations indicate that the increased temperature effect caused the replacement of HBD molecules by anions chloride around Co^{2+} ions for the SDW1 and SDW3 systems between the temperatures of 298 K to 353 K, except for the SDW2 system that the replaced occurred in the interval of 313 K to 353 K. Besides, the increase of temperature occasioned the increase of strength for Co-Cl interaction and weakened the interactions between the Co^{2+} ions with the oxygen of HBD molecules.

Keywords: Deep eutectic solvents; Cobalt; Electrochemical techniques; Computational simulations

1 Introduction

Deep eutectic solvents (DESs) are a mixture of organic salts that act as an acceptor of the hydrogen bond (HBA) with a molecule that acts as a donor of the hydrogen bond (HBD). The main property of DESs is the decrease in the melting point of the mixture concerning its respective isolated components pure, the reduction occurs by the displacement of charge present in the hydrogen bond between the halide ion with the compound that acts as HBD.[1]

Some physical and chemical properties of eutectic solvents are similar to ionic liquids (ILs),[1] however, ILs have a high cost, and the vast majority have low biodegradability and dangerous toxicity,[2] therefore, DESs is a promising alternative to replace ionic liquids. Besides, eutectic solvents have several advantages over organic solvents, such as non-toxicity, biodegradability, low vapor pressure, and high thermal stability.[3]

Furthermore, DESs are hygroscopic and the accumulation of water in these solvents can cause a significant change in its chemical structure and physicochemical properties.[4] For instance, our group[5,6] showed that the addition of water (ranged from 0.1 up to 10%) electrocatalyses the electrochemical reduction of Cu^{2+} and Ag^{+} species on the Pt surface from choline chloride and ethylene glycol at a molar ratio 1:2 (1ChCl:2EG) and choline chloride and urea at a molar ratio 1:2 (1ChCl:2U), respectively.

Due to these advantages concerning other solvents and liquids, the interest in DESs has been increasing in recent years in several areas, such as electrodeposition, and molecular modelling based on density functional theory (DFT) and molecular dynamics (MD) allow the comprehension of the interactions between the ionic metallic species with the solvent molecules. For instance, for Cu^{2+} in ethaline[5], MD simulations indicated that the water molecules replace the ethylene glycol molecules that were coordinated with Cu^{2+} ions, while the interactions between Cu^{2+} and Cl^{-} ions were not influenced by the presence of water. For Ag^{+} in reline[6], the MD calculations suggested that water molecules do not interact strongly with Ag^{++} ions but induce a small reduction in the number of urea molecules around of the ion and that the water molecules adjust to free spaces in the mixture.

Cobalt and cobalt-based alloys coatings are promising materials for applications including sensors,[7] biomedical applications,[8,9] electrocatalysis,[10] and antibacterial activity.[11] Co-based coatings can be prepared using high-vacuum techniques[12] such as chemical vapour deposition,[13] pulsed laser deposition[14] and sputtering,[15] among others. However, all these techniques require sophisticated equipment and/or high temperatures processes which increase the cost of the final product, making production on an industrial scale difficult. Alternative low-

cost techniques, such as hydrothermal methods[16,17] also have been used for the preparation of these materials, but long periods of synthesis and further heat treatments are needed.

In the present work, it is reported the effect of the temperature on the transport and electrochemical properties of Co^{2+} ions dissolved in three DESs (1ChCl:2EG, 1ChCl:2U and 1ChCl:2G). Furthermore, theoretical computational methodologies include classical mechanics by MD[18] and quantum mechanics by Bader's Quantum Theory of Atoms in Molecules (QTAIM)[19,20] were applied to understand the interaction between the Co^{2+} species with others chemical species present in the electrolytes.

2 Materials

2.1 Experimental methods

The reagents used were: choline chloride (ChCl, $HOC_2H_4N(CH_3)_3Cl$, Sigma-Aldrich, 98%), ethylene Glycol (EG, $HOCH_2CH_2OH$, Sigma-Aldrich, 99%), urea (U, $(NH_2)_2CO$, Sigma-Aldrich, 99%), and glycerol (G, $C_3H_5(OH)_3$, J.T Baker, 99%). All reagents were used as received without further purification. Eutectic mixtures were prepared following the methodology described by Abbott *et al.*[21] The reagents were mixed in a 1:2 molar ratio (1ChCl:2EG, 1ChCl:2U and 1ChCl:2G) and heated to 353 K until a homogeneous, colourless liquid formed.

The amount of water in DES mixtures was monitored over 7 (seven) days in ambient conditions by Karl-Fischer Titration (Metrohm-Eco Chemie), and the results showed that after this interval of time the water content did not exceed 25 ppm, as can be seen in Fig. S1 (in †ESI), which corresponds to 0.0025%. After obtaining the eutectic mixtures, $CoCl_2$ was added to obtain an electroplating solution containing 0.1 mol L^{-1} $CoCl_2$ ($CoCl_2.6H_2O$, Sigma-Aldrich, 98%).

All electrochemical experiments were performed in a three-electrode electrochemical cell under air at 298 K, 313 K, 333 K, and 353 K. The electrochemical data were obtained from a potentiostat/galvanostat (AUTOLAB PGSTAT30, Metrohm-Eco Chemise) controlled by NOVA 2.1 software. The pseudo-reference was Ag/AgCl immersed in the corresponding DESs. A Pt plate (1 cm^2) was used as the counter-electrode, and a Cu disc, with a diameter of 0.18 cm was used as the working electrode. Before each electrochemical experiment, the working electrode was sanded with emery paper from 400 up to 1200 mesh. Furthermore, the cleaning procedure was applied to all Cu electrodes before the coating depositions: degreasing in 10 % NaOH solution, rinsing in Milli-Q water, quickly immersed in 10 % HCl solution, rinsed again in Milli-Q water and, finally air-dried.

The cyclic voltammograms (CVs) were recorded for each investigated temperature between -0.7 V and -1.2 V at 10 mV s^{-1}. The diffusion coefficients (*D*) of the Co^{2+} specie in the three DESs were determined by the chronoamperometry technique, applying a potential step from a region where there was no faradaic process, to a region of diffusional control of the reduction of the Co^{2+} species. The current transients were adjusted with the Cottrell equation, Equation 1:

$$I(t) = \frac{nFAD_O^{\frac{1}{2}}C}{(\pi t)^{\frac{1}{2}}} \quad (1)$$

where *I* is the current (A), *n* is the number of electrons involved in the process, *F* is the Faraday constant (96 485 C mol^{-1}), *A* is the electrode geometric area (cm^2), *D* is the diffusion coefficient (cm^2 s^{-1}), C is the concentration of the species in solution (mol L^{-1}) and t is the time (s).

The viscosity and specific mass measurements of the eutectic electroplating solutions containing 0.1 mol L^{-1} $CoCl_2.6H_2O$, were performed on an Anton Paar Stabinger viscometer, model SVM 3000, at the following working temperatures, 298 K, 313 K, 333 K, and 353 K.

2.2 Simulation methods

The Density Functional Theory (DFT) [22] was utilized in the optimize in the gas phase of HBD molecules (ethylene glycol, urea, and glycerol) and choline ion, through of hybrid functional B3LYP [23] and the base set 6-311G+(d,p),[24] from the GAUSSIAN 09 package.[25] After optimization, the Multiwfn *software* [26] was used to obtain partial charges through CHELPG method [27] for some components of the system (ethylene glycol, urea, glycerol, and choline). Fig. 1 showed the structures used in the MD simulations and the nomenclature of main atoms studied

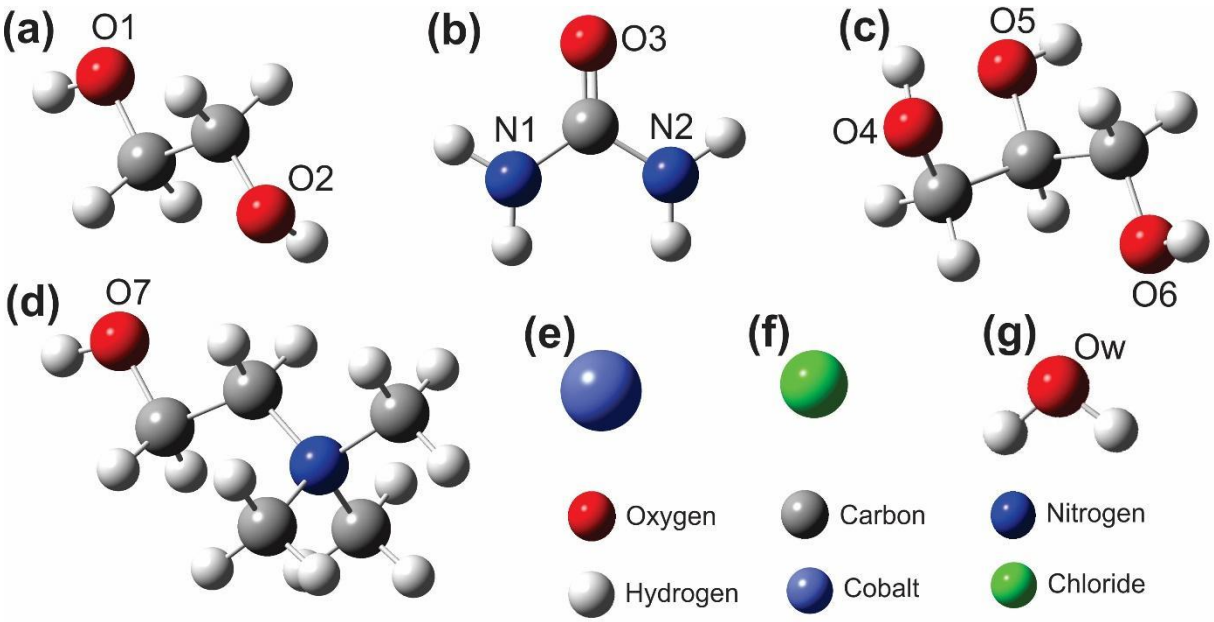

Fig. 1 Structures used in the MD simulations and nomenclature of main atoms. (a) ethylene glycol, (b) urea, (c) glycerol, (d) choline, (e) cobalt, and (f) chloride.

All MD simulations were realized by using Gromacs 2020.4 package.[28] 800 HBD molecules, 400 choline ions, 418 chloride ions, 9 cobalt ions, and 54 water molecules were added in the cubic box of simulation with dimensions of 8 nm × 8 nm × 8 nm for simulate in the temperatures of 298 K, 313 K, 333 K, and 353 K. Table 1 shows the number and the components present in each system.

Table 1 Number of molecules and ions present in each system used in MD simulations

Systems		
SDW1	**SDW2**	**SDW3**
Ethylene glycol (800)	Urea (800)	Glycerol (800)
Choline (400)	Choline (400)	Choline (400)
Chloride (418)	Chloride (418)	Chloride (418)
Cobalt (9)	Cobalt (9)	Cobalt (9)
Water (54)	Water (54)	Water (54)

The force field chosen to describe the systems was OPLSS-AA.[29] The parameters used to describe cobalt were obtained by L. Zhao *et al.*[30] The geometry of systems was optimized through the steepest descent algorithm [31] for 100.000 steps with an energy tolerance of 10 kJ mol^{-1} nm^{-1} and step size of 10^{-4} nm. Subsequently, 10 ns equilibrium dynamics with NVT and

NPT ensembles were realized. The first one was performed using the V-rescale method [32] in temperatures of 298 K, 313 K, 333 K, and 353 K for each system. For the NPT ensemble, the system pressure was controlled using a Parrinelo-Rahman barostat [33] in the value of 1.0 bar. Finally, 200 ns production MD was performed through of Leap-Frog algorithm [34] with a time step of 2.0 fs. The protocol and an example of the input file of production MD are available (in †ESI).

The QTAIM was employed to obtain deeper insight into the interactions between Co^{2+} ions with each system investigated.[19,20] The equilibrium structures from 200 ns MD simulations were chosen as a starting point for the QTAIM calculations. Only components within a 5.0 Å radius from the cobalt ion were considered for the calculations. Thereafter, single-point calculations were performed at B3LYP hybrid functional.[23] The LanL2DZ [35] and SDD [36] effective core potentials (ECP) along with their valence basis set were used for cobalt ion, and 6-31+G(d,p) basis set for the C, Cl^-, H, N, and O atoms by using GAUSSIAN 09 package [25] including the electron density which was further used for QTAIM calculations. All topological information and Electron Localization Function (ELF)[37] analysis were calculated by Multiwfn *software*.[26]

3 Results

3.1 Experimental results

Cyclic voltammetry was used to obtain the working electrochemical potential range of the investigated eutectic mixtures at different temperatures. The CVs obtained for all the investigated solvents, without Co addition, are shown in Fig. S2 (in †ESI). No electrochemical process was observed in the CVs obtained from 1ChCl:2EG and 1ChCl:2G. However, an electrochemical process at about –1.2 V vs Ag/AgCl, attributed to the electrochemical reduction of water [38] is observed in the CVs obtained from 1ChCl:2U.

CVs for the electrochemical reduction of Co on Cu are shown in Fig. 2. During the forward scan, a single peak, related to the electrochemical reduction of Co^{2+}/Co, appears in all the CVs. It is especially well-defined for 1ChCl:2U, since for both 1ChCl:2EG and 1ChCl:2G, Co electrodeposition occurs simultaneously with the electrochemical reduction of both solvents, but for 1ChCl:2U, Co electrodeposition takes place in a potential region that is free from the electrochemical reduction of the solvent. The electrochemical reductions of the three eutectic solvents are attributed to the reduction of choline ions (Ch^+), as well as hydroxyl groups (EG and G), and traces of water.[39,40] Furthermore, an increase in the bath temperature leads to an increase in the peak current, which is related to the decrease of the electrolyte viscosity

(Table S1, in †ESI) with temperature and the corresponding increase in the diffusion coefficient of Co^{2+} (Table S2, in †ESI). Thus, these CVs (Fig. 2) suggest that Co electrodeposition is more efficient in 1ChCl:2U than in the others two electrolytes. Furthermore, these CVs also show current loops between the forward and reverse scans (except for the CVs obtained from 1ChCl:2G solutions at 298 K and 313 K), which indicate that nucleation plays an important role in Co electrodeposition on Cu.

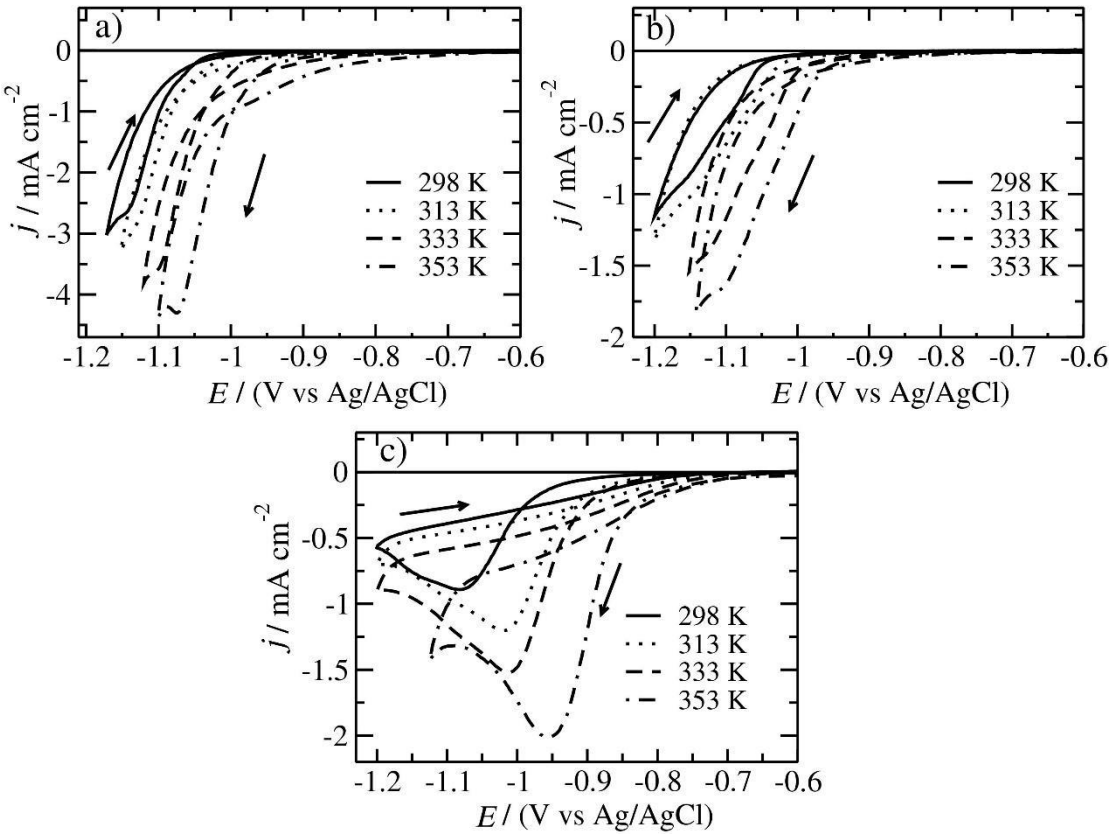

Fig. 2 Cyclic voltammograms obtained on Cu electrode in (a) 1ChCl:2EG, (b) 1ChCl:2G, and (c) 1ChCl:2U containing 0.1 mol L^{-1} $CoCl_2.6H_2O$ at several temperatures. Scan rate of 10 mV s^{-1}.

The diffusion coefficients (*D*) of the Co^{2+} species were calculated by the well-known Cottrell method. The experimental current-time curves are shown in Figs. S3-S5 (in †ESI) were fitted by the Cottrell equation (Equation 1). The values of the diffusion coefficients obtained for Co^{2+} species in DESs by this method are listed in Table S2 (in †ESI). These results are an average of three experiments, and the mean value for each diffusion coefficient is shown with its standard deviation. Comparing the Co^{2+} diffusion coefficients obtained from the three studied DESs, at the same temperature, it is clear that the Co^{2+} diffusion coefficient is

significantly higher for 1ChCl:2EG, which also has the lowest viscosity values (Table S1, in †ESI). Moreover, all diffusion coefficients increased as the bath temperature increased, which also suggests an improvement in the mass transport as the electrolyte viscosity decreases with temperature. Table S1 (in †ESI) shows the values dynamic viscosity (η) of the three electroplating solutions at different temperatures. The increase in the bath temperature from 298 K up to 353 K promoted a decrease in viscosity, as expected for regular liquids (Table S1, in †ESI).

The temperature dependence of the Co^{2+} species diffusion coefficients was well fitted by a equation similar to that of Arrhenius (Equation 2).

$$lnD = lnD_0 - \frac{E_D}{k_B}T \qquad (2)$$

In equation 2, D_0 is a constant, k_B is the Boltzmann constant, T is the absolute temperature and E_D is the apparent activation energies for the diffusion of the Co^{2+} species. From the fitted gradient, E_D values of 15.3, 29.9, and 55.2 kJ mol^{-1} for 1ChCl:2EG, 1ChCl:2U, and 1ChCl:2G, respectively, were calculated. The higher activation energy values presented by 1ChCl:2G indicate that the mass transport in this solvent encounters a higher energy barrier (and also requires a higher consumption of electric energy) in comparison to the 1ChCl:2EG and 1ChCl:2U electrolytes.

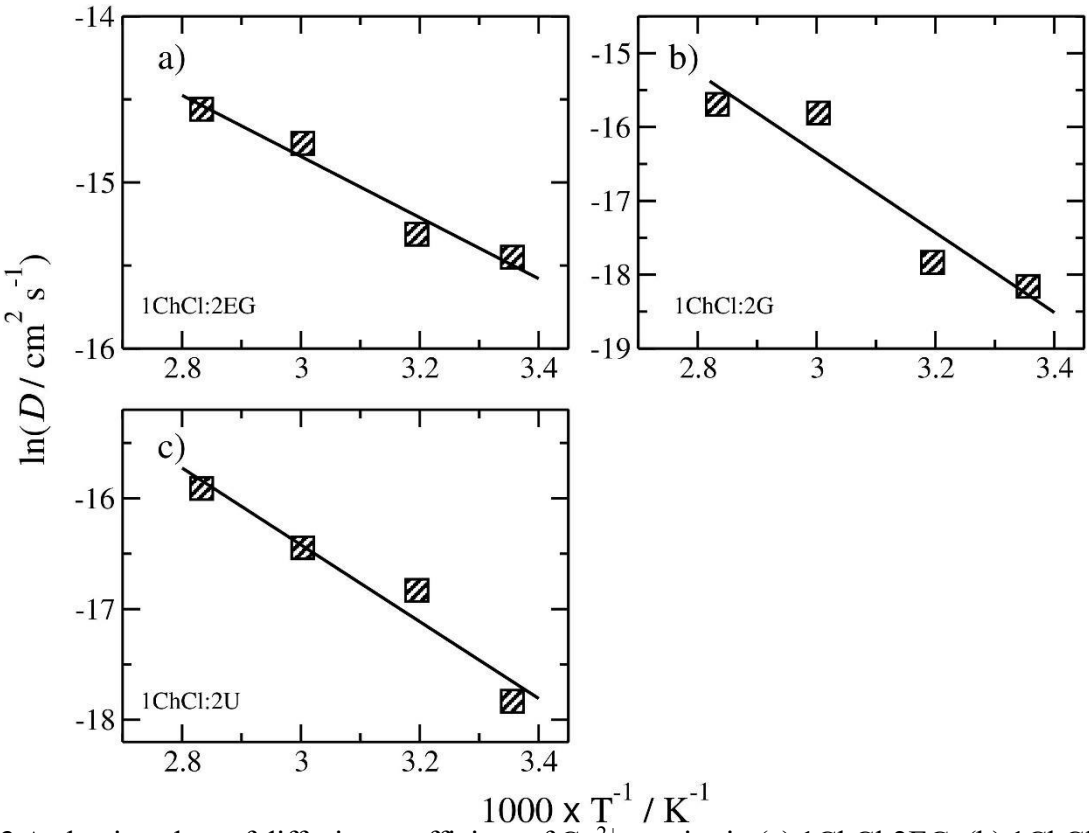

Fig. 3 Arrhenius plots of diffusion coefficient of Co^{2+} species in (a) 1ChCl:2EG, (b) 1ChCl:2G, and (c) 1ChCl:2U.

The Stokes–Einstein equation (Equation 3) describes the diffusion of spherical particles through a liquid of low Reynolds number:

$$D = \frac{k_B T}{6\pi\eta a} \quad (3)$$

where k_B is the is the Boltzmann constant, T is the absolute temperature and a is the solvodynamic radius. It has been applied to other non-aqueous electrochemical systems. For example, Rogers and co-workers [41] used it to describe the behaviour of cobaltocenium hexafluorophosphate and ferrocene in several room temperature ionic liquids (RTILs), while Huang *et al.*[42] studied how well it applies to the diffusion of small molecules such as H_2S and SO_2 in RTILs.

It was assessed whether Equation 3 describes the relationship between the Co^{2+} diffusion coefficient and the DESs viscosity by plotting D against T/η and the found relationships are shown in Fig. 4. As seen from Fig. 4, all plots display the linear relatioship between D and T/η, enabling us to calculate effective values of a of 0.95, 1.06, and 0.70 nm for

1ChCl:2EG, 1ChCl:2U, and 1ChCl:2G, respectively. All three DESs yielded physically reasonable values close to 1 nm. However, such values are high in comparison with effective ionic radius of Co^{2+} in crystalline structure (0.058 - 0.09 nm),[43] suggesting that dissolved Co^{2+} ions in the eutectic mixtures could be coordinated with complexing agents.

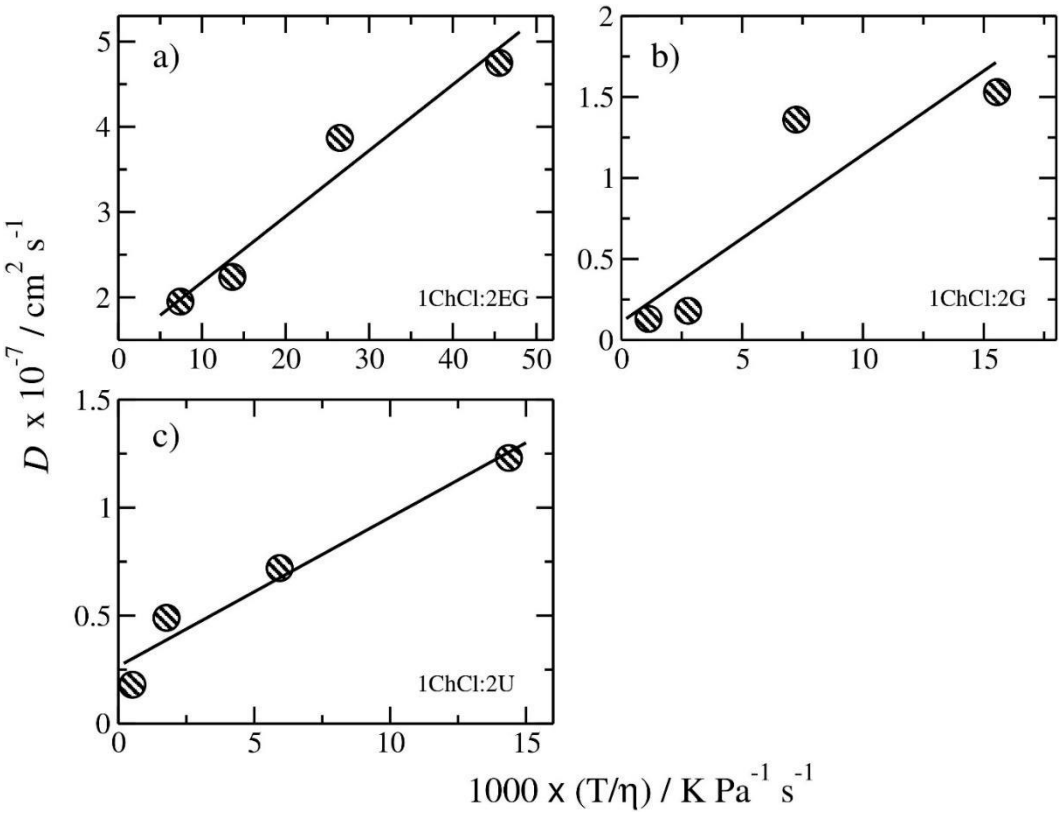

Fig. 4 Stokes-Einstein plots obtained from (a) 1ChCl:2EG, (b) 1ChCl:2G, and (c) 1ChCl:2U.

3.2 Computational results

3.2.1 Validation of MD simulations

To validate the systems simulated through of OPLS-AA force field and CHELPG method is necessary to correlate the data of specific mass (Fig. 5) and diffusion coefficient (Fig. 6) obtain by experimental and theoretical methods. Fig. 5 showed the values of specific mass in function of temperature for the SDW1 (Fig. 5a), SDW2 (Fig. 5b), and SDW3 (Fig. 5c) systems. Analyzing the increasing temperature effect, occurred the reduction of specific mass in the three systems simulated (Fig. 5a, 5b, and 5c) for two methods (experimental and theoretical) analyzed. The diffusion coefficient values are present in Fig. 6 for the same systems analyzed previously (Fig. 6a, 6b, and 6c). Analyzing the increasing temperature effect, was observed the increase of values for the diffusion of coefficient. Therefore, OPLS-AA force field and CHELPG method may be used to describe the interactions presents in the systems.

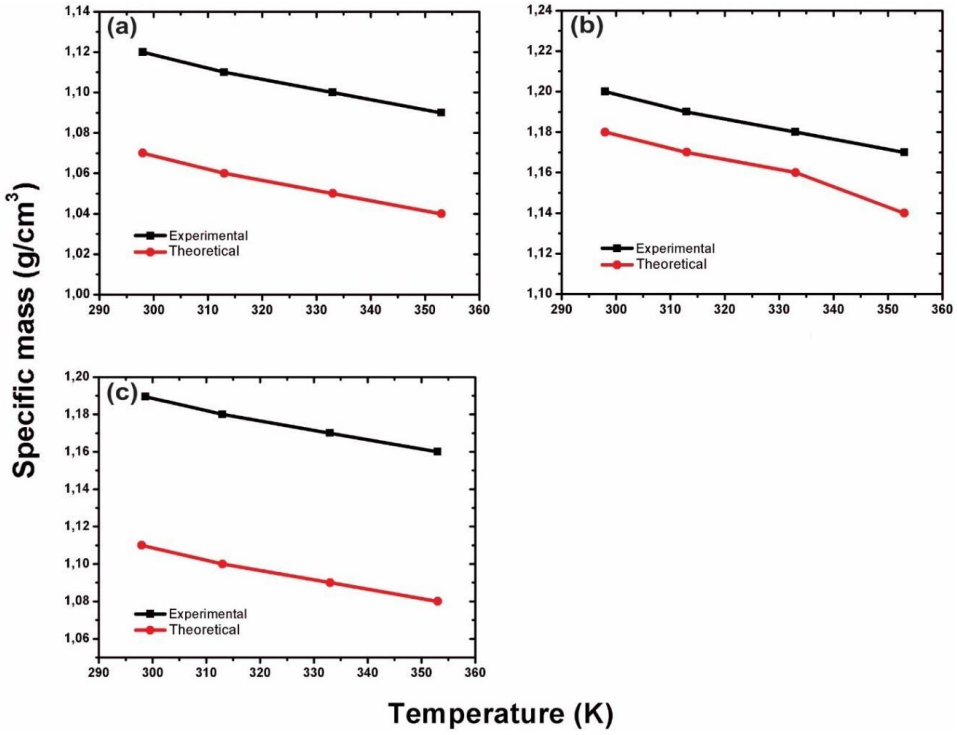

Fig. 5 Correlation between the values of specific mass obtain though of experimental and theoretical methods in function of temperature. Systems simulated: (a) SDW1, (b) SDW2, and (c) SDW3.

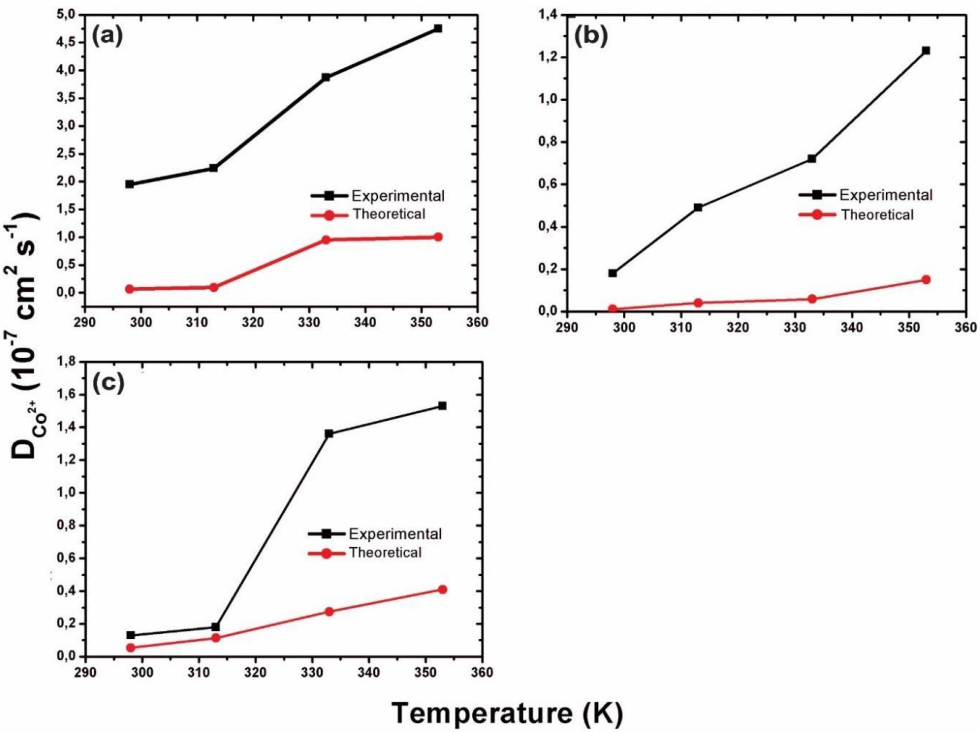

Fig. 6 Correlation between the diffusion coefficient obtain though of experimental and theoretical methods in function of temperature. Systems simulated: (a) SDW1, (b) SDW2, and (c) SDW3.

3.2.2 Co^{2+} ions in the SDW1 system

Fig. 7 shows the radial distribution function (RDF) that performs a structural analysis of the system through probability density of the components around the Co^{2+} ions at temperatures 298 K, 313 K, 333 K, and 353 K (Figs. 7a, 7b, 7c, and 7d, respectively). The RDF results shown in Fig. 7 indicated that the main interaction is between Co^{2+} ions and the anions chloride around 3.50 Å independent of temperature; the high value of g(*r*) for Co-Cl interaction is explained due a strong attraction electrostatic between these ions. The second and third strongest interactions were Co-Ow and Co-(O1,O2), respectively. Both interactions showed a distance with Co^{2+} ions in the values around 3.10 Å independent of temperature. Due to the lowest g(*r*) value for Co-O7, the interaction of Co^{2+} ions with choline oxygen (O7) was disregarded. Analyzing the increasing temperature effect, the probability of Co^{2+} ions interact with anion chloride becomes bigger due to the increase in the value of g(r) for the temperatures of 333 K and 353 K (Fig.7c and 7d, respectively). On the other hand, there are a decrease significative in the g(*r*) values for Co-Ow and Co-(O1,O2) interactions for the temperatures of 333 K and 353 K (Fig.7c and 7d, respectively).

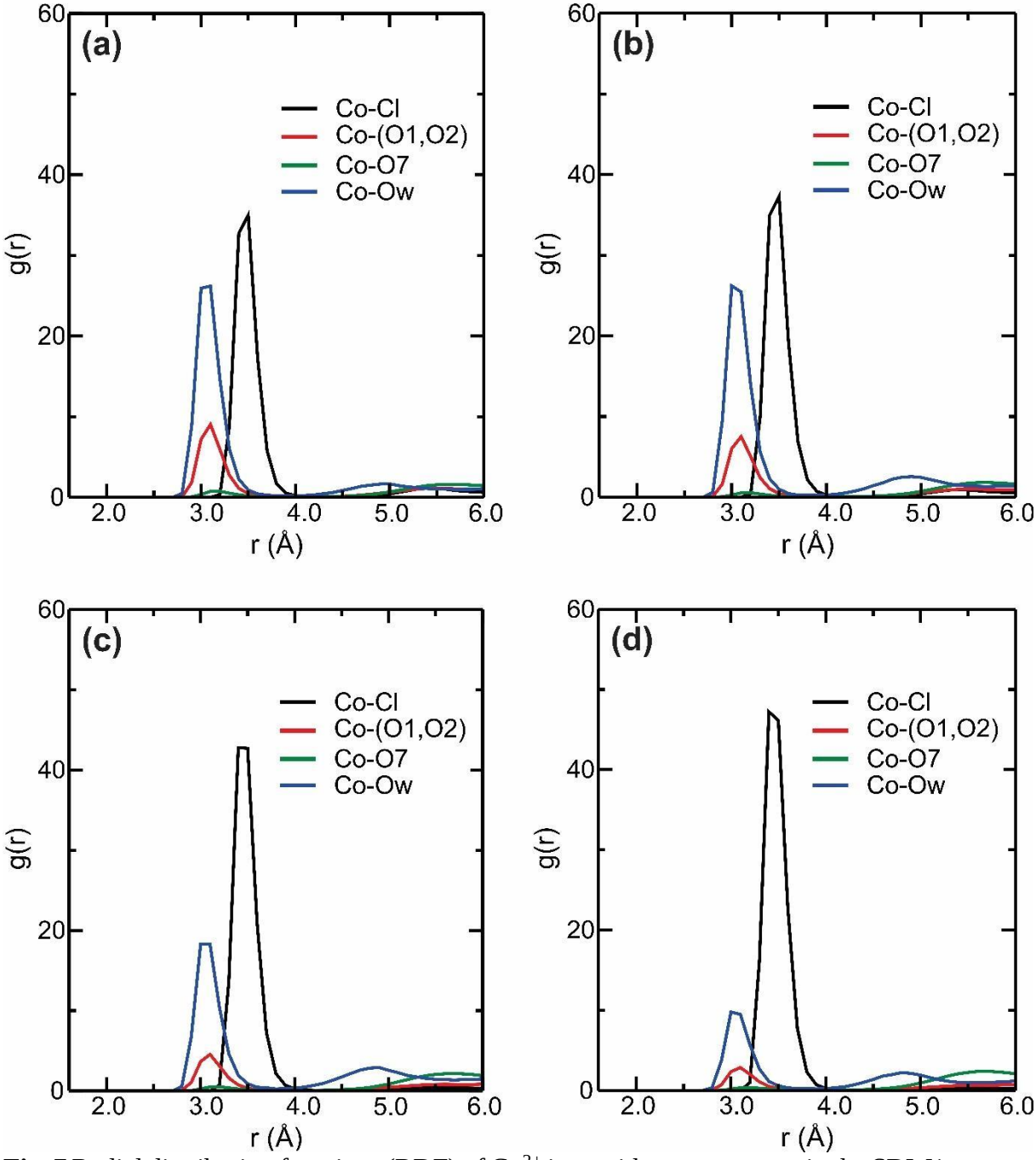

Fig. 7 Radial distribution functions (RDF) of Co^{2+} ions with atoms present in the SDW1 system, at temperatures (a) 298 K, (b) 313 K, (c) 333 K, and (d) 353 K.

Fig. 8 shows the cumulative number (CN) between Co^{2+} ions with anion chloride (Fig. 8a), ethylene glycol (Fig. 8b), and water (Fig. 8c) molecules in the function of distance. Analyzing the temperatures of 298 K and 353 K [which are extreme values of the graph for Co-Cl and Co-(O1,O2) interactions in the Figs 8a and 8b, respectively], the value of CN increase of 3.8 for 5.3 to Co-Cl interaction (Fig. 8a), while that for Co-(O1,O2) interaction (Fig. 8b) occurred the reduction of CN (3.4 for 1.1) for the respective temperatures. The Co-Ow

interaction (Fig. 8c) shows values of CN similar for the four temperatures (298 K, 313 K, 333 K, and 353 K). Analyzing the increasing temperature effect, the results indicate that the replacement of ethylene glycol molecules by anion chloride around Co^{2+} ions in the temperature range from 298 K to 353 K.

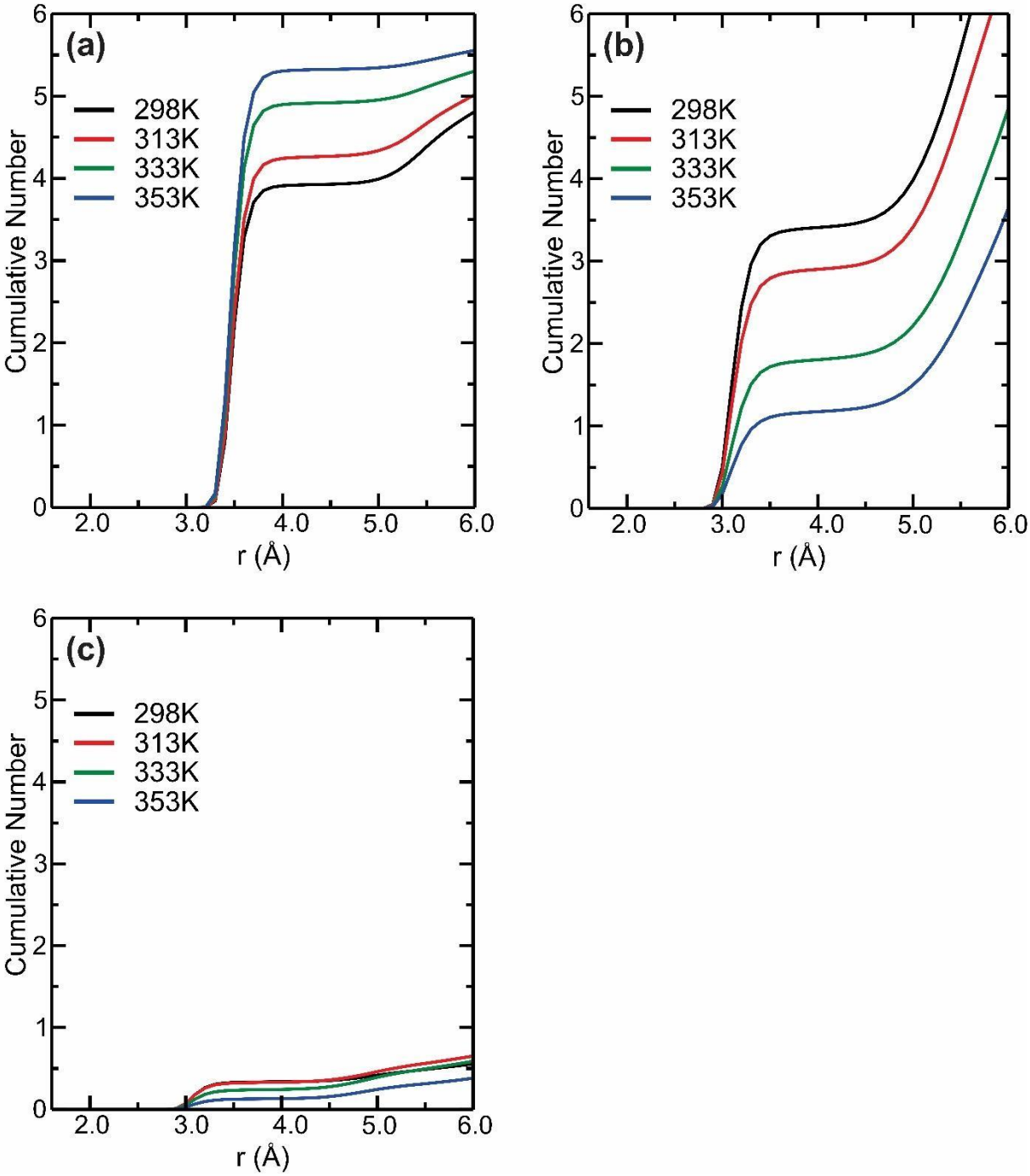

Fig. 8 Cumulative number (CN) of (a) Co-Cl, (b) Co-(O1, O2), and (c) Co-Ow interactions.

The spatial distribution function (SDF) present in Fig. 9 shows how the components of the system are distributed around Co^{2+} ions in the temperature of 298 K (Fig. 9a) and 353 K

(Fig. 9b); these interval temperatures that occurred the replaced of ethylene glycol molecules by anions chloride around Co^{2+} ions (Fig. 8a and 8b). In the temperature of 298 K (Fig. 9a) and 353 K (Fig. 9b), anion chloride (green) showed a strong predominance around Co^{2+} ions (red), following ethylene glycol (blue) and water (yellow) molecules. Analyzing increasing temperature effect, occurred the increase of density for anion chloride (green) around Co^{2+} ions, while ethylene glycol molecules dispersed and distanced. The density of the water remains almost constant around Co^{2+} ions.

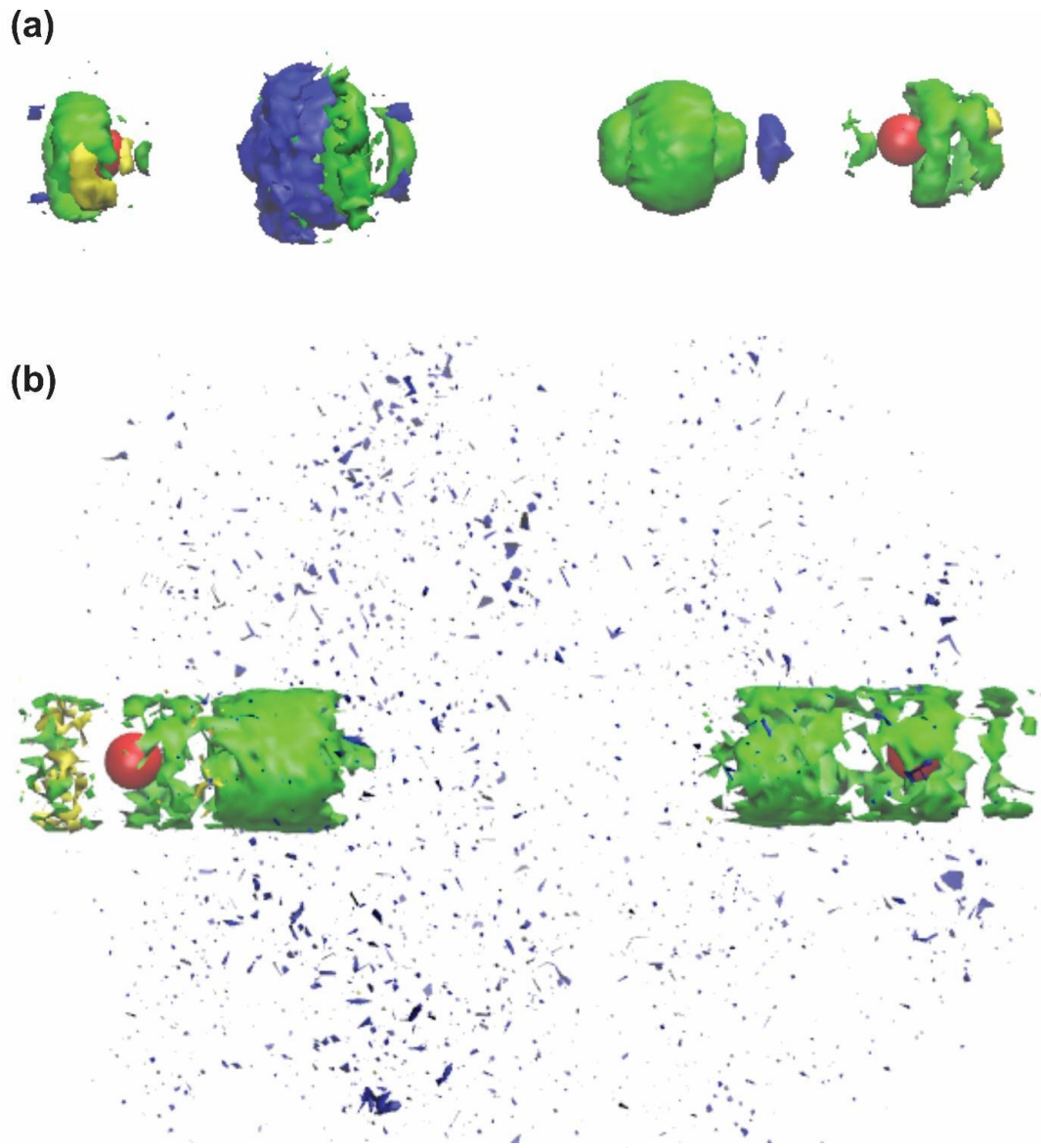

Fig. 9 Spatial distribution function (SDF) between Co^{2+} ions with components present in the SDW1 system, at temperatures (a) 298 K and (b) 353 K. Co^{2+} (red); chloride (green, isovalue = 0.0013); ethylene glycol (blue, isovalue = 0.0105); water (yellow, isovalue = 0.0004).

Table 2 Topological data for Co^{2+} interactions with SDW1 system, at temperatures of 298 K and 353 K. Electron density, ρ(r), Laplacian of electron density, $\nabla^2\rho$(r), ELF value, η(r), at bond critical points (BCP) of selected Co-Cl and Co-(O1,O2) interactions.

Interaction	BCP	ρ(r)	$\nabla^2\rho$(r)	η(r)	Temperature
Co-Cl	1	4.4178E-03	5.6272E-03	3.5801E-02	298 K
	2	4.8021E-03	5.4073E-03	4.2747E-02	
	3	5.3218E-03	5.9067E-03	5.1373E-02	
Co-(O1,O2)	4	2.7309E-03	6.7171E-03	8.4408E-03	
	5	4.1283E-03	1.0764E-02	1.3462E-02	
	6	7.4588E-03	1.7342E-02	3.0535E-02	
	7	8.8611E-03	3.5664E-02	2.2609E-02	
	8	7.0132E-03	2.8131E-02	1.7752E-02	
	9	5.5279E-03	1.0170E-02	2.5343E-02	
Co-Cl	1	6.4179E-03	9.5046E-03	5.3092E-02	353 K
	2	9.0937E-03	1.7924E-02	6.6055E-02	
	3	5.7288E-03	7.9153E-03	4.7295E-02	
	4	3.9595E-03	5.4928E-03	2.7936E-02	
Co-(O1,O2)	5	8.1720E-03	2.7091E-02	2.3503E-02	
	6	5.0484E-03	1.0710E-02	1.8471E-02	
	7	4.4691E-03	1.5122E-02	1.2072E-02	
	8	5.71817E-03	1.4260E-02	2.0113E-02	

Table 2 contains values of the electronic density, *ρ(r)*, the Laplacian of the electronic density, $\nabla^2\rho(r)$, and the electron localization function (ELF), *η(r)*, for Bond Critical Points (BCPs) of Co^{2+} with the SDW1 system. The sum of all ρ(r) values for Co-Cl interaction in the temperatures of 298 K and 353K were of $\Sigma\rho$(r) = 1.4542E-02 and $\Sigma\rho$(r) = 2.5200E-02, respectively. As well as the sum of η(r) values for the above interaction and in the same temperatures were of $\Sigma\eta$(r) = 1.2992E-01 and $\Sigma\eta$(r) = 1.9438E-01, respectively. On the other hand, the Co-(O1,O2) interaction registered in the temperatures of 298 K and 353 K the sum of

all ρ(r) values were of $\Sigma\rho$(r) = 3.5720E-02 and $\Sigma\rho$(r) = 2.3408E-02, respectively. While that the sum of η(r) values were of $\Sigma\eta$(r) = 1.1814E-01 and $\Sigma\eta$(r) = 7.4159E-02, in the same temperatures above, respectively. Therefore, the increasing temperature occasioned an increase in the strength of Co-Cl interaction, while that the Co-(O1,O2) interaction became weaker. Moreover, the positive values of $\nabla^2\rho$(r) indicate that the electronic density is locally depleted characterizing intra or intermolecular interactions. [44] The molecular graphs with bond paths and the interactions [Co-Cl and Co-(O1,O2)] are illustrated in Figs. 10a and 10b in the temperatures of 298 K and 353 K, respectively.

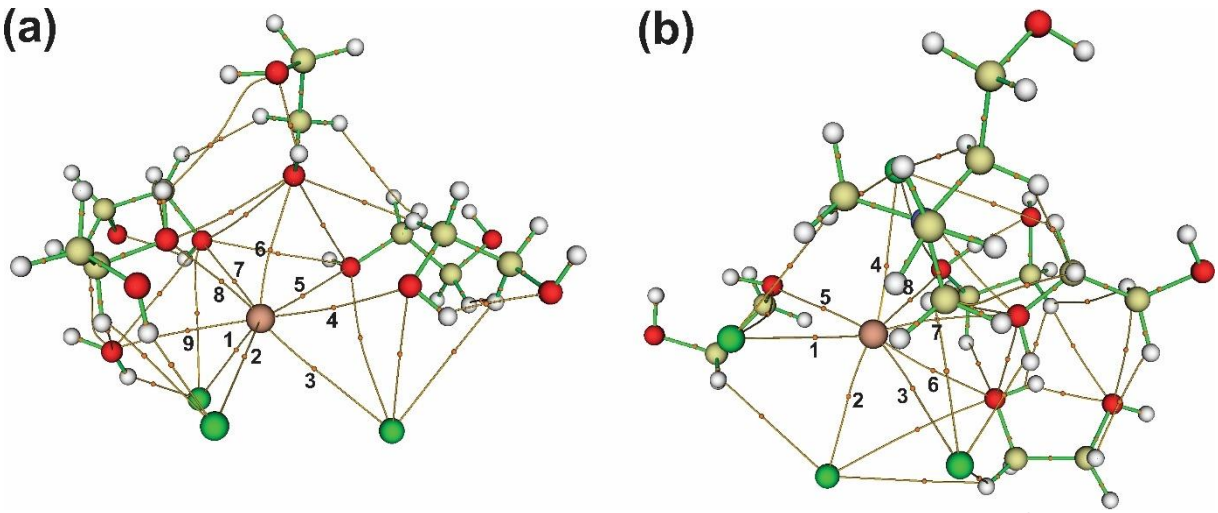

Fig. 10 Molecular graphs with intramolecular interactions and BCP of the Co^{2+} ion with the SDW1 system, at temperatures of (a) 298 K and (b) 353 K.

3.2.2 Co^{2+} ions in the SDW2 system

The RDF plot present in Fig. 11 showed that the main interaction was between the Co^{2+} ions with anion chloride around 3.50 Å independent of temperature; this high value of g(*r*) is explained by the strong attraction electrostatic between these ions. The second and third strongest interactions were between the Co^{2+} ions with the urea oxygen (O3) and water oxygen (Ow), respectively; both interactions present in the same distance of 3.10 Å independent of temperature. The others interactions [Co-(N1,N2) and Co-O7] will not be discussed due to their low g(*r*) value. Analyzing the increasing temperature effect, the probability of Co-Cl and Co-O3 interactions did not show changes significative due to the value of g(r) remain almost constant (Figs. 11a, 11b, 11c, and 11d). On the other hand, the probability for Co-Ow interaction increased due to the increase of g(*r*) in the temperature of 313 K and 333 K (Figs. 11b and 11c, respectively).

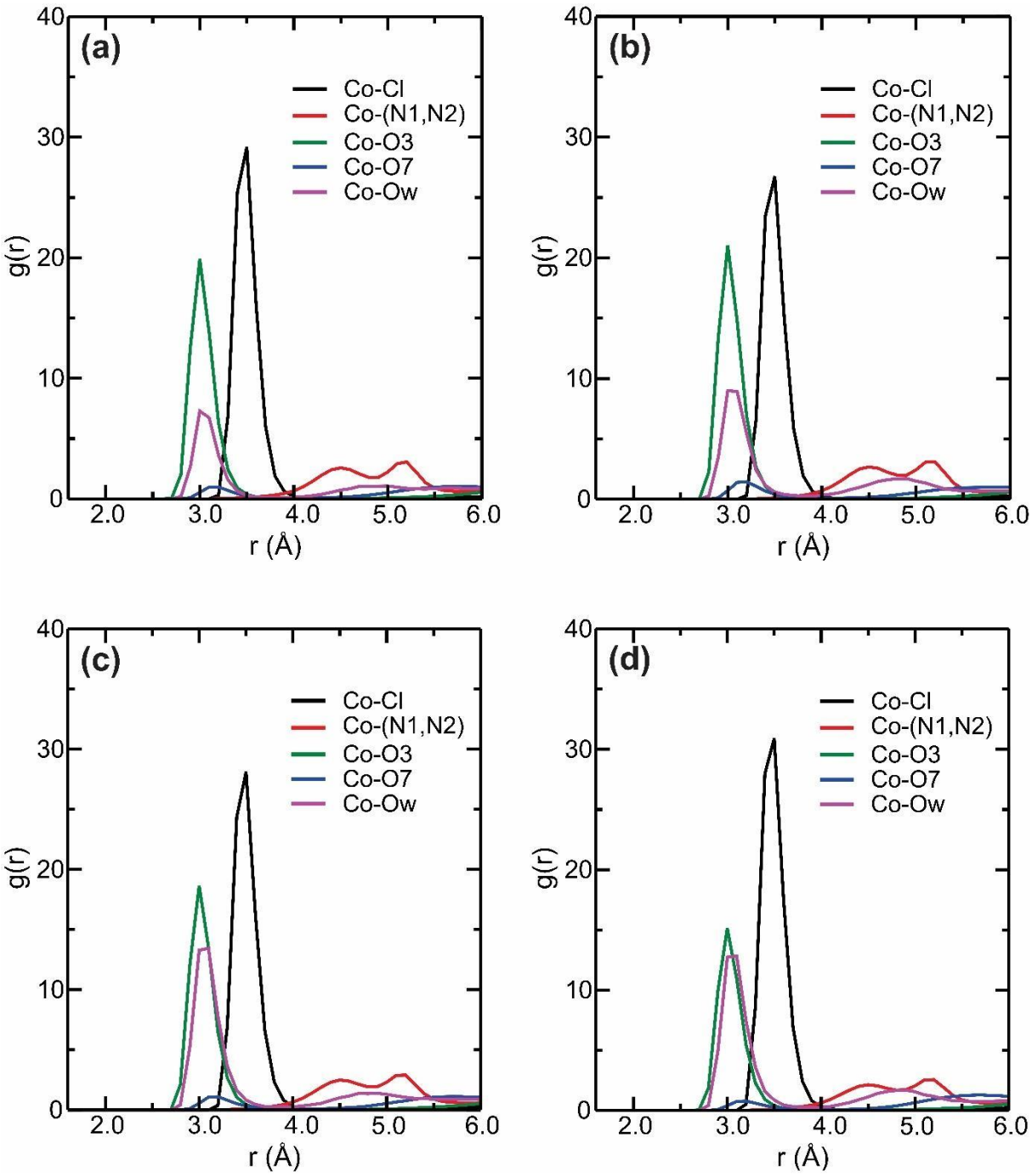

Fig. 11 Radial distribution functions (RDF) of Co^{2+} ions with atoms present in the SDW2 system, at temperatures (a) 298 K, (b) 313 K, (c) 333 K, and (d) 353 K.

Analyzing the values of CNs (Fig. 12) in the temperature of 313 K to 353 K (that are extremes values of the plots for Co-Cl and Co-O3 interactions), Co-Cl interaction (Fig. 12a) showed an increase from 3.45 to 4.10, while that the Co-O3 interaction (Fig. 12b) showed a reduction from 3.87 to 2.90. The Co-Ow interaction (Fig. 12c) remains similar values of CN in

the four temperatures (298 K, 313 K, 333 K, and 353 K). Analyzing the increasing temperature effect in the interval of 313 K to 353 K, the replaced occurred of urea molecules by anion chloride around Co^{2+} ions.

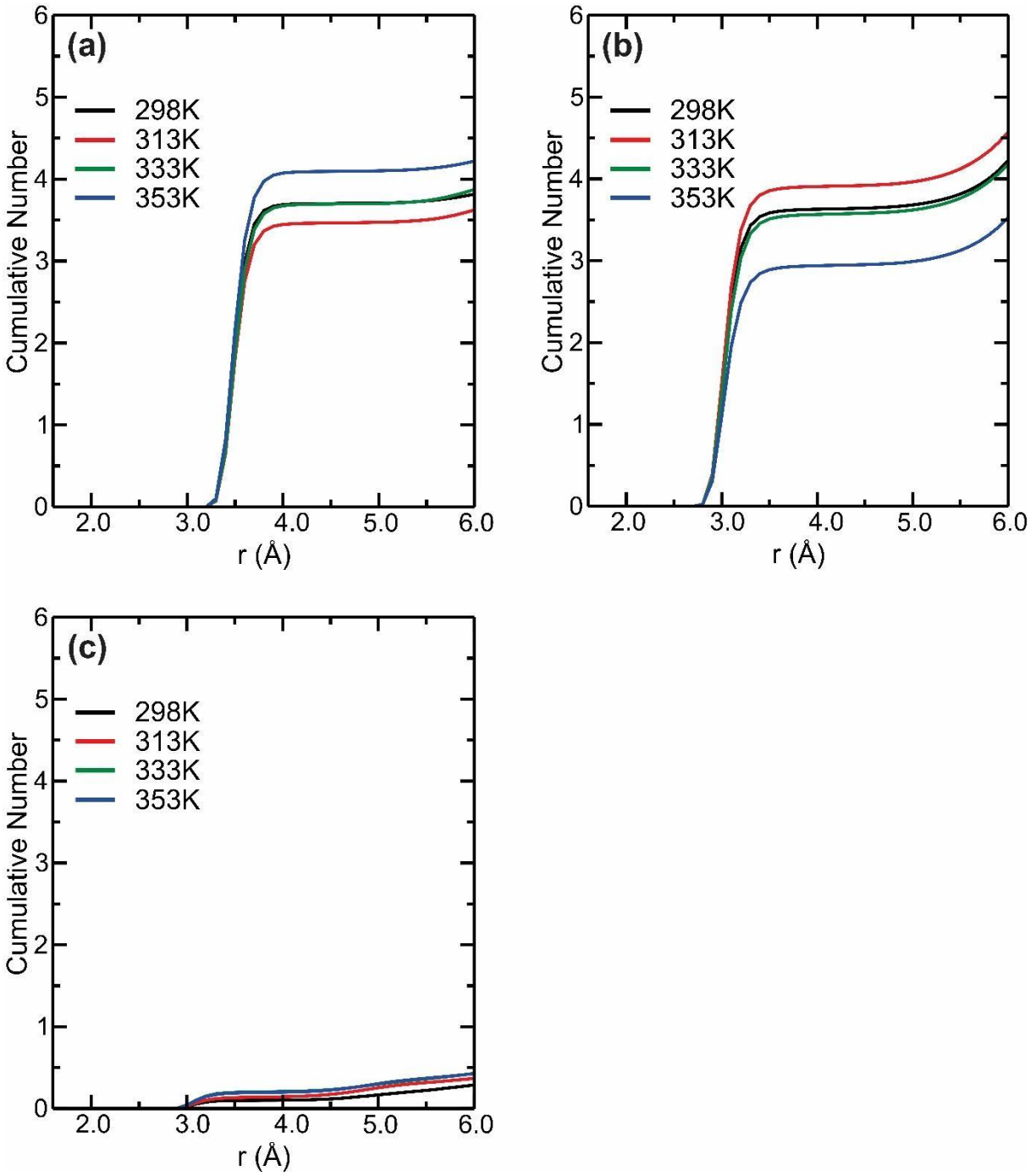

Fig. 12 Cumulative number (CN) of (a) Co-Cl, (b) Co-O3, and (c) Co-Ow interactions.

Analyzing the SDFs in the temperatures of 313 K (Fig. 13a) and 353 K (Fig. 13b), the density of chloride (green) is mainly distributed around of Co^{2+} ions than that urea (blue) and

water (yellow) molecules. The temperatures of 313 K and 353 K were chosen due to the replacement of urea molecules by anions chloride around the Co^{2+} ions occurring in these intervals of temperature (Figs. 12a and 12b). Analyzing the increasing temperature effect, the density of anion chloride increased around Co^{2+} ions while the density of urea molecules decreased. On the other hand, the density of water molecules did not show changes significant with the increasing temperature effect.

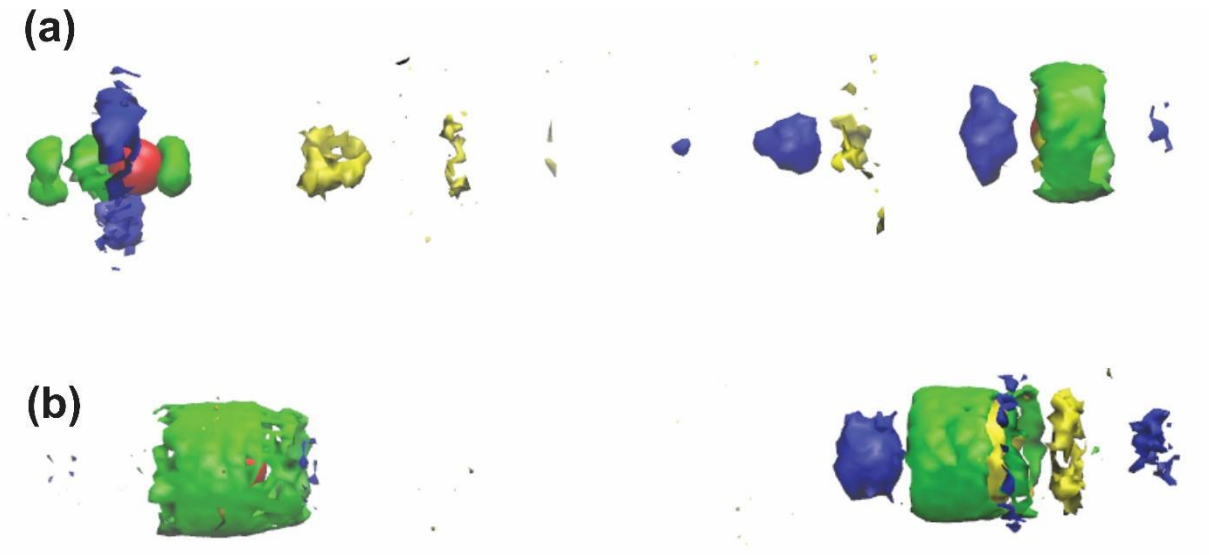

Fig. 13 Spatial distribution function (SDF) between Co^{2+} ions with components present in the SDW2 system, at temperatures (a) 313 K and (b) 353 K. Co^{2+} (red); chloride (green, isovalue = 0.0038); urea (blue, isovalue = 0.0127); water (yellow, isovalue = 0.0007).

Table 3

Topological data for Co^{2+} interactions with SDW2 system, at temperatures of 313 K and 353 K. Electron density, ρ(r), Laplacian of electron density, $\nabla^2\rho$(r), ELF value, η(r), at bond critical points (BCP) of selected Co-Cl and Co-O3 interactions.

Interaction	BCP	ρ(r)	$\nabla^2\rho$(r)	η(r)	Temperature
Co-Cl	1	7.1075E-03	9.3280E-03	6.3513E-02	313 K
	2	4.6003E-03	6.9248E-03	3.3827E-02	
Co-O3	3	7.3932E-03	2.4596E-02	2.2047E-02	
	4	7.7985E-03	2.7305E-02	2.3869E-02	
	5	5.0633E-03	1.0495E-02	1.8503E-02	
	6	6.5064E-03	2.1060E-02	2.0054E-02	
	7	6.0316E-03	1.2461E-02	2.4420E-02	
	8	7.3798E-03	1.9579E-02	2.4314E-02	
	9	2.6162E-03	7.1097E-03	6.5241E-03	
Co-Cl	1	5.7570E-03	1.0509E-02	3.9428E-02	353 K
	2	6.2899E-03	9.9886E-03	4.8826E-02	
	3	6.9508E-03	1.3194E-02	4.8486E-02	
	4	5.7448E-03	7.8832E-03	4.5789E-02	
Co-O3	5	6.9977E-03	1.8893E-02	2.4500E-02	
	6	8.1299E-03	2.2050E-02	2.7215E-02	
	7	5.2635E-03	1.5281E-02	1.5865E-02	

The topological data referring to the BCP of interactions between Co^{2+} ions and the SDW2 system are present in Table 3. Analyzing the temperatures of 313 K and 353 K for Co-Cl interaction, the sum of the values of ρ(r) were of Σρ(r) = 1.1708E-02 and Σρ(r) = 2.4743E-02, for the respective temperatures, as well as the sum of all η(r) were of Ση(r) = 9.7340E-02 and Ση(r) = 1.8253E-01, for the respective temperatures. Performing the same analysis in the same temperature ranges for the Co-O3 interaction, the sum of the values ρ(r) were of Σρ(r) = 4.2789E-02 and Σρ(r) = 2.0391E-02, as well as the sum of the values of η(r) were of Ση(r) =

1.3973E-01 and $\Sigma\eta(r)$ = 6.7580E-02, for the respective temperatures. Therefore, the increasing temperature occasioned in the increase of strength for Co-Cl interaction, in comparison that the Co-O3 interaction became weaker. Moreover, positive values of $\nabla^2\rho(r)$ indicate that intra or intermolecular interactions are present because the electronic density is locally depleted.[44] The molecular graphs with bond paths and BCP at temperatures 313 K and 353 K are shown in Figs. 14a and 14b, for Co-Cl and Co-O3 interactions, respectively.

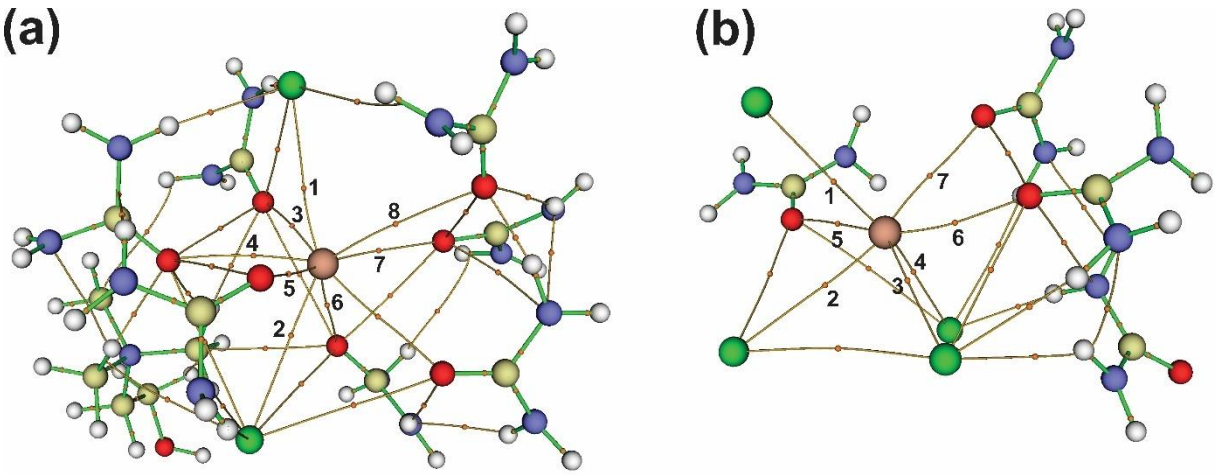

Fig. 14 Molecular graphs with intramolecular interactions and BCP of the Co^{2+} ion with the SDW2 system, at temperatures of (a) 313 K and (b) 353 K.

Co^{2+} ion in the SDW3 system

Fig. 15 shows a strong interaction between the Co^{2+} ions and the anion chloride around 3.50 Å independent of temperature; the high value of g(*r*) for this interaction is explained due to the strong attraction electrostatic between these ions. The second and third strongest interactions were Co-Ow and Co-(O4,O5,O6), respectively; both interactions are localized around 3.10 Å independent of temperature. The Co-O7 interaction will not be discussed due to the low value of g(*r*) showed. Analyzing the increasing temperature effect, the probability of Co-Cl interaction (Figs. 15a, 15b, 15c, and 15d) showed a slight increase while that for Co-(O4,O5,O6) and Co-Ow interactions (Figs. 15a, 15b, 15c, and 15d) showed a small reduction.

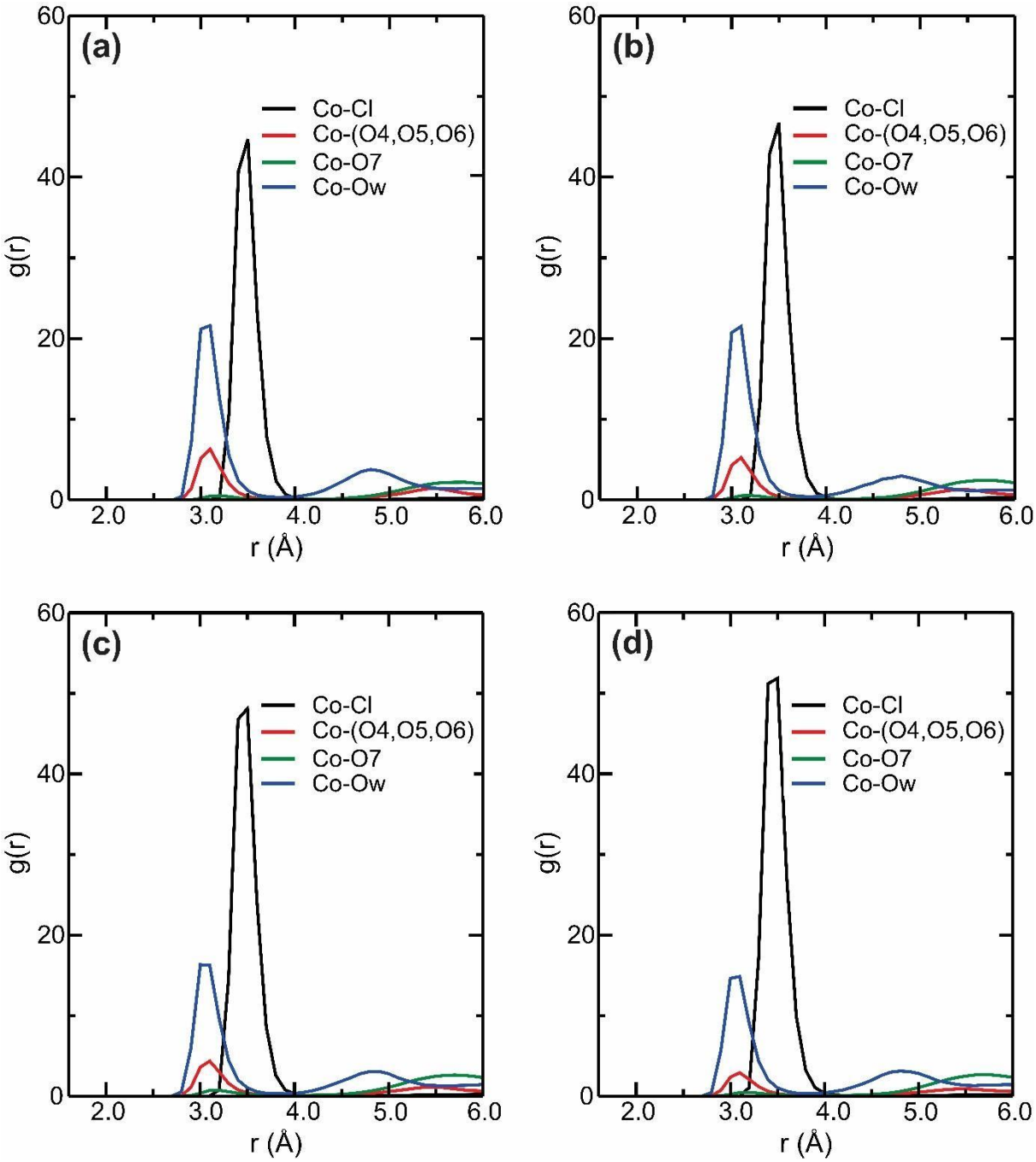

Fig. 15 Radial distribution functions (RDF) of Co^{2+} with atoms present in the SDW3 system, at temperatures (a) 298 K, (b) 313 K, (c) 333 K, and (d) 353 K.

The CNs (Fig.16) were analyzed in the temperatures of 298 K and 353 K due to were extremes values of the plots for Co-Cl and Co-(O4,O5,O6) interactions (Figs 16a and 16b, respectively). The Co-Cl interaction showed an increase of 4.25 to 5.20 while the Co-(O4,O5,O6) interaction presented a reduction of 3.0 to 1.5, in the respective temperatures (298K and 353 K). On the other hand, g(*r*) values for Co-Ow interaction (Fig. 16c) showed were

similar independent of temperature. Analyzing the increasing temperature effect, occurred a replacement of glycerol molecules by anions chloride around of Co^{2+} ions.

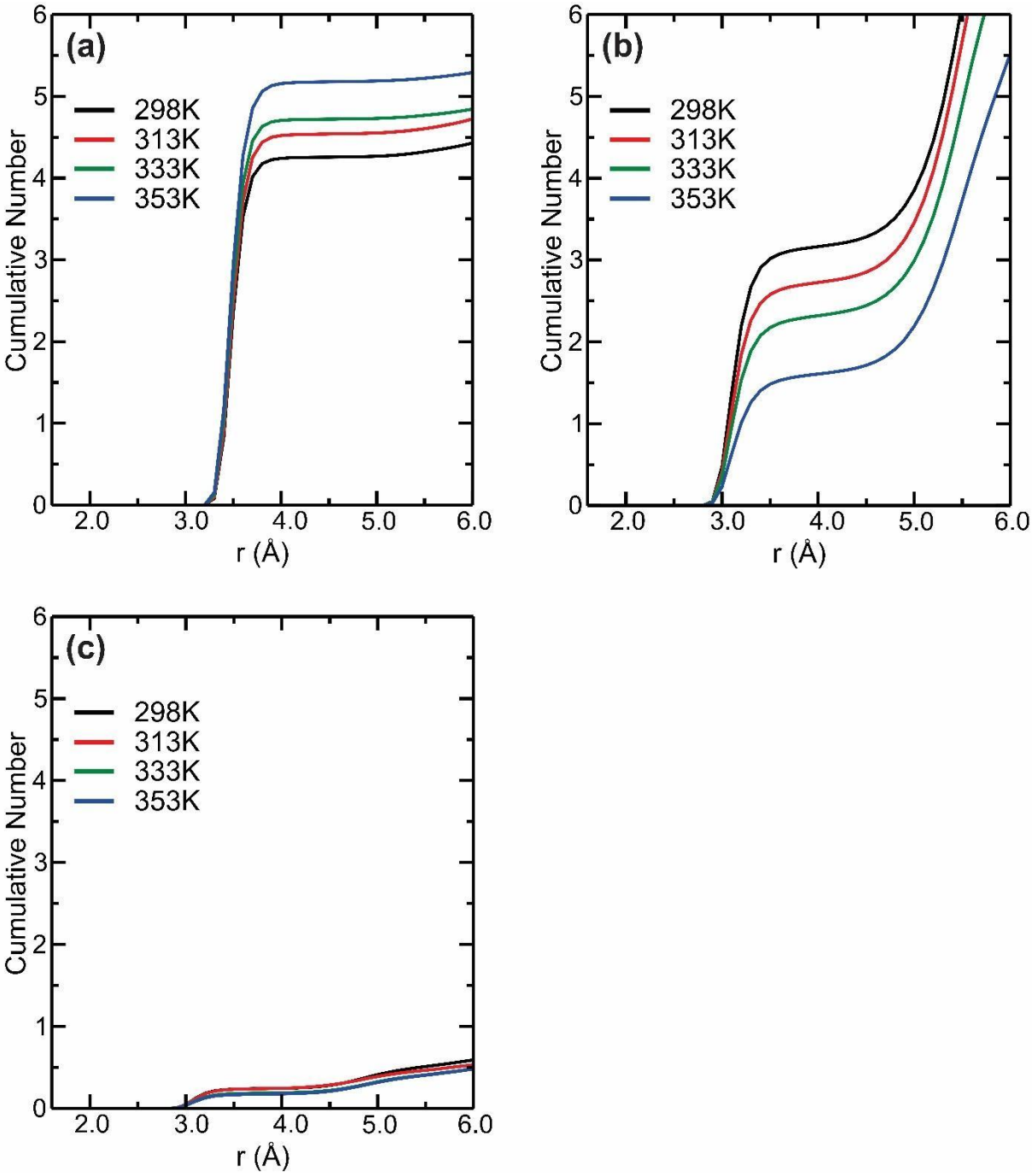

Fig. 16 Cumulative number (CN) of (a) Co-Cl, (b) Co-(O4,O5,O6), and (c) Co-Ow interactions.

The SDFs in the temperatures of 298 K (Fig. 17a) and 353 K (Fig. 17b) showed a high distribution of density of anion chloride (green) around Co^{2+} ions, following glycerol (blue) and water (yellow) molecules. These temperatures were chosen due to the replacement of glycerol

molecules by anion chloride (Fig. 16a and 16b) occur in this interval (298K to 353K). Analyzing the increasing temperature effect, the density of anion chloride becomes more pronounced around Co^{2+} ions while that the density of urea molecules spread in the system. On the other hand, the density of the water remains almost constant around Co^{2+} ions.

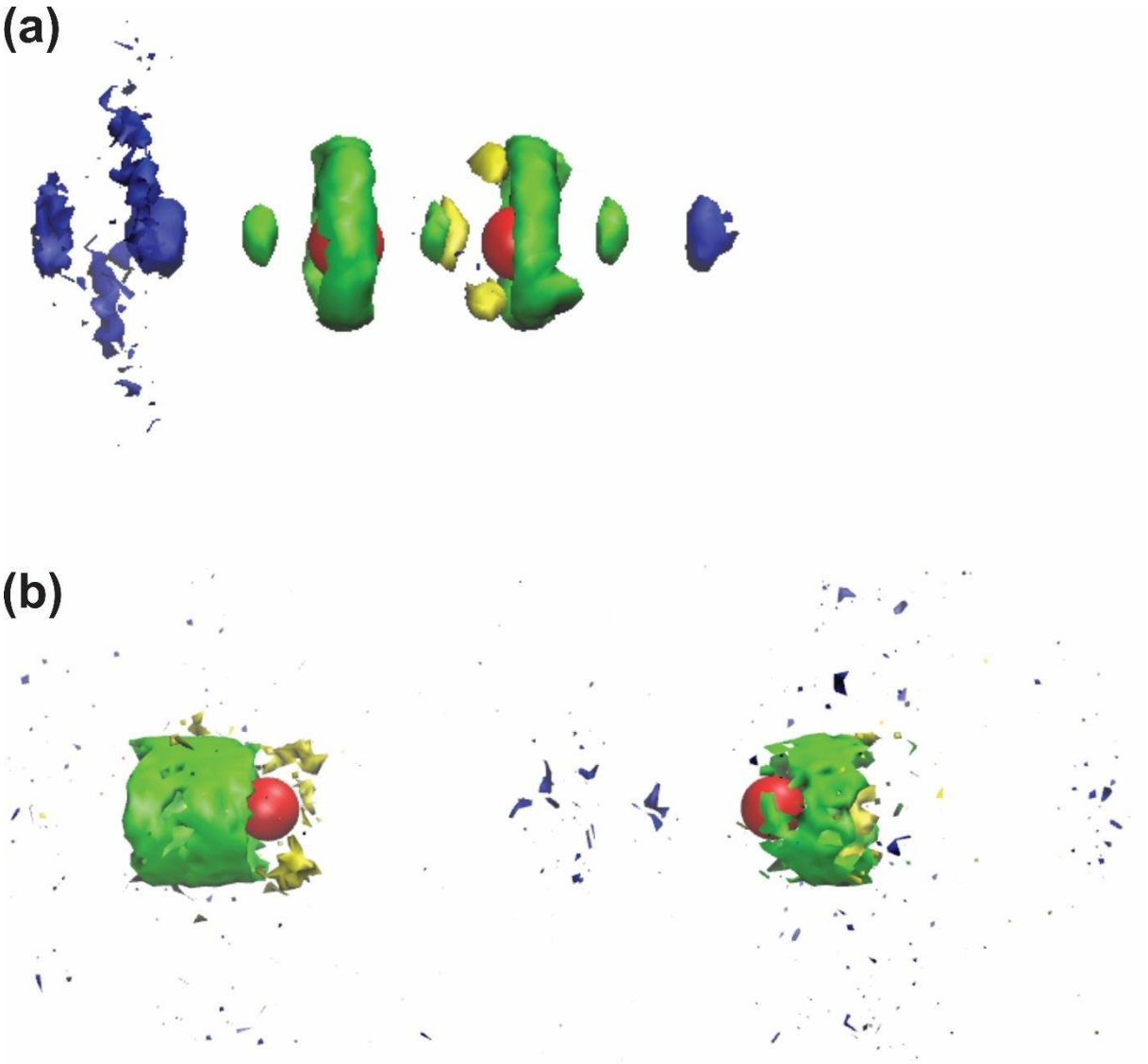

Fig. 17 Spatial distribution function (SDF) between Co^{2+} ions with components present in the SDW3 system, at temperatures (a) 298 K and (b) 353 K. Co^{2+} (red); chloride (green, isovalue = 0.0047); glycerol (blue, isovalue = 0.0122); water (yellow, isovalue = 0.0027).

Table 4

Topological data for Co^{2+} interactions with SDW3 system, at temperatures of 298 K and 353 K. Electron density, ρ(r), Laplacian of electron density, $\nabla^2\rho$(r), ELF value, η(r), at bond critical points (BCP) of selected Co-Cl and Co-(O4,O5,O6) interactions.

Interaction	BCP	ρ(r)	$\nabla^2\rho$(r)	η(r)	Temperature
Co-Cl	1	1.0766E-03	6.1057E-03	1.0380E-03	298 K
	2	8.8393E-03	1.6326E-02	6.7860E-02	
	3	4.6079E-03	5.1647E-03	4.1799E-02	
Co-(O4,O5,O6)	4	3.8872E-03	1.0373E-02	1.2066E-02	
	5	6.1783E-03	1.8120E-02	2.0318E-02	
	6	6.5377E-03	1.7995E-02	2.3707E-02	
	7	6.3158E-03	1.5833E-02	2.1769E-02	
Co-Cl	1	6.0489E-03	9.1343E-03	4.8536E-02	353 K
	2	6.2926E-03	8.6926E-03	5.4145E-02	
	3	7.6925E-03	1.2531E-02	6.4176E-02	
	4	7.8102E-03	1.3716E-02	6.0627E-02	

Table 4 shows the topological data of Co^{2+} interaction with the SDW3 system, the sum of all ρ(r) values for Co-Cl interaction were of $\Sigma\rho$(r) = 1.4524E-02 and $\Sigma\rho$(r) = 2.7844E-02, in the temperatures of 298 K and 353K, respectively. As well as the sum of all η(r) for the same interaction above were of $\Sigma\eta$(r) = 1.1070E-01 and $\Sigma\eta$(r) = 2.2748E-01, for the same temperatures analyzed. On the other hand, the Co-(O4,O5,O6) interaction showed ρ(r) and η(r) values only in the temperature of 298 K that were $\Sigma\rho$(r) = 2.2919E-02 and $\Sigma\eta$(r) = 7.7860E-02, while that in the temperature of 353 K the SDW3 system did not present BCP with Co^{2+} ions. Therefore, the increasing temperature occasioned in the increase of strength for Co-Cl interaction, while that the Co-(O4,O5,O6) interaction presents a reduction in the number of BCP. $\nabla^2\rho$(r) values positive were registered indicate that intra or intermolecular interactions are present in this system,[44] indicate that the electronic charges are depleted along the interatomic path, being a characteristic of closed-shell interactions.[45] Fig. 18a and 18b show the molecular graphs with bond paths and BCP of Co-Cl and Co-(O4,O5,O6) interactions, at temperatures of 298 K and 353 K, respectively.

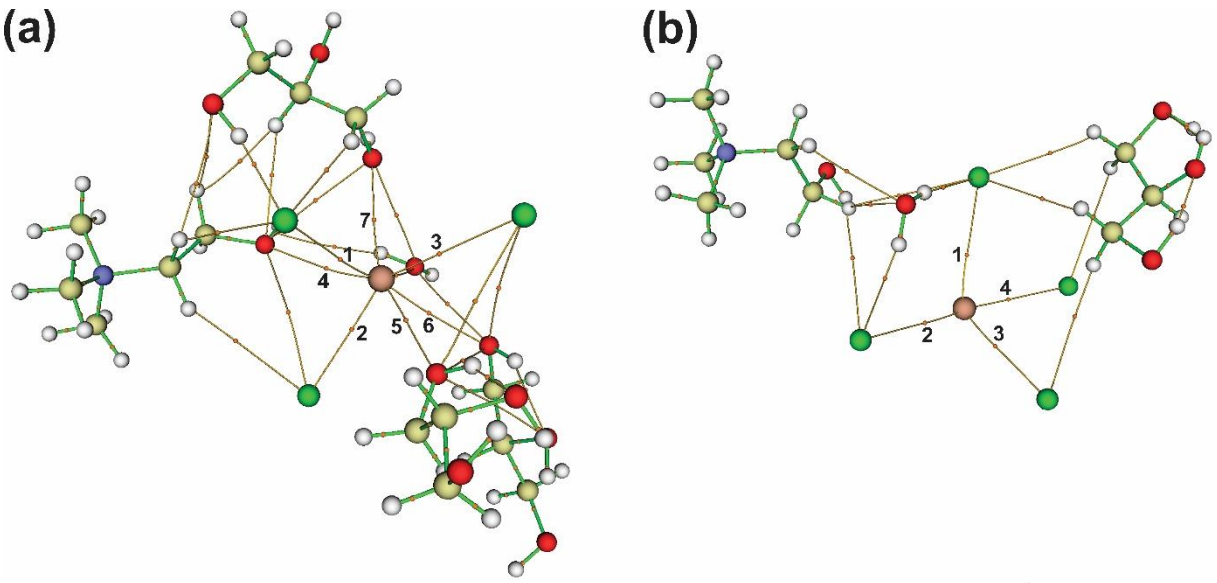

Fig. 18 Molecular graphs with intramolecular interactions and BCP of the Co^{2+} ion with the SDW3 system, at temperatures of (a) 298 K and (b) 353 K.

4 Conclusions

For all three electrolytes, the increase in the diffusion coefficient and decrease in the viscosity with increasing temperature was clearly apparent. The relationship could be quantified via the Cottrell and Arrhenius equations. Calculated values of the activation energies showed that energy barriers for the diffusion of Co^{2+} ions followed the following sequence: 1ChCl:2EG < 1ChCl:2U < 1ChCl:2G.

The simulations by molecular dynamics (MD) showed a strong interaction of anion chloride with Co^{2+} ions independent of temperature in the three systems analyzed. Besides, in the interval of temperature between 298 K and 353 K occurred the replaced of HBD molecules by anion chloride around Co^{2+} ions for SDW1 and SDW3 systems, while for SDW2 system this replaced occurred between 313 K and 353 K. The CN between Co^{2+} ions with water molecules did not showed changes significative with the increase temperature effect in the three systems analyzed. The simulations realized by QTAIM indicated that the Co-Cl interaction became stronger due to the increase of temperature in the three systems (SDW1, SDW2, and SDW3) analyzed. In contrast, the increase in temperature weakened the interaction between Co^{2+} ions with the oxygen of HBD molecules.

Author contributions

Lucas Lima Bezerra: methodology, validation, formal analysis, writing – original draft. Francisco Gilvane Sampaio Oliveira: investigation, methodology, writing – reviewing and editing. Luis Paulo Mourão dos Santos: methodology, writing – reviewing and editing. Hosiberto Batista de Sant'Ana: resources, writing – reviewing & editing. Filipe Xavier Feitosa: investigation. Adriana Nunes Correia: resources, writing – reviewing & editing. Walther Schwarzacher: writing – reviewing & editing. Emmanuel Silva Marinho: writing – reviewing & editing. Pedro de Lima-Neto: conceptualization, resources, writing – reviewing & editing. Norberto Kássio Vieira Monteiro: supervision, writing – reviewing & editing.

Supplementary material

The supplementary material includes CVs and Cottrellian profiles experimentally obtained for all the investigated solvents. Experimental diffusion coefficients and viscosity are shown in the Tables S1 and S2, respectively.

Conflicts of interest

The authors report no declarations of interest.

Acknowledgments

The authors thank the financial support given by the following Brazilian funding agencies: Coordenação de Aperfeiçoamento de Pessoal de Nível Superior (CAPES), Conselho Nacional de Desenvolvimento Científico e Tecnológico (CNPq) and Fundação Cearense de Apoio ao Desenvolvimento Científico e Tecnológica (FUNCAP). Pedro de Lima-Neto and Adriana N. Correia thank the financial support received from CNPq projects: 408626/2018-6, 304152/2018-8, Adriana N. Correia thanks the financial support received from CNPq projects: 305136/2018-6, 405596/2018-0. Lucas. L. Bezerra, Francisco G. S. Oliveira and Luis P. M. dos Santos thank CAPES for their scholarship. The authors are grateful to the Centro Nacional de Processamento de Alto Desempenho (CENAPAD) of the Federal University of Ceará (UFC) by computational resources offered.

Data availability

The data that supports the findings of this study are available within the article [and its supplementary material].

References

1. E. L. Smith, A. P. Abbott and K. S. Ryder, *Chem. Rev*, 2014, **114**, 11060-11082.

2. Q. Zhang, K. De Oliveira Vigier, S. Royer and F. Jérôme, *Chem. Soc. Rev*, 2012, **41**, 7108-7146.

3. P. S. Bangde, R. Jain and P. Dandekar, *ACS Sustain. Chem. Eng*, 2016, **4**, 3552-3557.

4. Y. Chen and T. Mu, *Green Chem. Eng*, 2021, **2**, 174-186.

5. J. R. Bezerra-Neto, N. G. Sousa, L. P. M. Dos Santos, A. N. Correia and P. De Lima-Neto, *Phys. Chem. Chem. Phys*, 2018, **20**, 9321-9327.

6. J. R. Bezerra-Neto, L. L. Bezerra, N. G. Sousa, L. P. M. dos Santos, E. S. Marinho, N. K. V. Monteiro, A. N. Correia and P. de Lima-Neto, *J. Mol. Model*, 2020, **26**, 339.

7. Y. Li, L. Shi, X. Cai, H. Zhao, X. Niu and M. Lan, *Electrochim. Acta*, 2019, **294**, 304-311.

8. J. Lim and S. A. Majetich, *Nano Today*, 2013, **8**, 98-113.

9. S. M. Ansari, R. D. Bhor, K. R. Pai, D. Sen, S. Mazumder, K. Ghosh, Y. D. Kolekar and C. V. Ramana, *Appl. Surf. Sci.*, 2017, **414**, 171-187.

10. C. Xu, Z. Lin, D. Zhao, Y. Sun, Y. Zhong, J. Ning, C. Zheng, Z. Zhang and Y. Hu, *J. Mater. Sci.*, 2019, **54**, 5412-5423.

11.Y. A. Syed Khadar, A. Balamurugan, V. P. Devarajan, R. Subramanian and S. Dinesh Kumar, *J. Mater. Res. Technol.*, 2019, **8**, 267-274.

12. V. G. Bayev, J. A. Fedotova, J. V. Kasiuk, S. A. Vorobyova, A. A. Sohor, I. V. Komissarov, N. G. Kovalchuk, S. L. Prischepa, N. I. Kargin, M. Andrulevičius, J. Przewoznik, C. Kapusta, O. A. Ivashkevich, S. I. Tyutyunnikov, N. N. Kolobylina and P. V. Guryeva, *Appl. Surf. Sci.*, 2018, **440**, 1252-1260.

13. D. X. Ye, S. Pimanpang, C. Jezewski, F. Tang, J. J. Senkevich, G. C. Wang and T. M. Lu, *Thin Solid Films*, 2005, **485**, 95-100.

14. J. H. Kim, H. Kim, D. Kim, Y. E. Ihm and W. K. Choo, *J. Appl. Phys.*, 2002, **92**, 6066-6071.

15. W. C. Chang, C. C. Lin, H. W. Chang, C. H. Chiu and S. K. Chen, *Surf. Coatings Technol.*, 2006, **200**, 3366-3369.

16. X. He, H. Yang, Z. Chen and S. S. Y. Liao, *Phys. B Condens. Matter*, 2012, **407**, 2895–2899.

17. M. Bastianello, S. Gross and M. T. Elm, *RSC Adv.*, 2019, **9**, 33282-33289.

18. N. H. Morgon and K. R. P. P.-S. P. Coutinho, 2007.

19. H. J. Bohórquez, R. J. Boyd and C. F. Matta, *J. Phys. Chem. A*, 2011, **115**, 12991-12997.

20. (a) R.F.W. Bader, *Acc. Chem. Res*, 1985, **18**. (b) R.F.W. Bader, *Acc. Chem. Res*, 1991, **91.**

21. A. P. Abbott, D. Boothby, G. Capper, D. L. Davies and R. K. Rasheed, *J. Am. Chem. Soc*, 2004, **126**, 9142-9147.

22. C. F. Zinola, Electrocatalysis, 2010, 664.

23. J. P. Perdew, K. Burke and M. Ernzerhof, *Phys. Rev. Lett*, 1996, **77**, 3865–3868.

24. M. J. Frisch, J. A. Pople and J. S. Binkley, *J. Chem. Phys*, 1984, **80**, 3265-3269.

25. M. J. Frisch. *et al*. Gaussian 09, Revision B.01Gaussian 09, Revision B.01, Gaussian, Inc., Wallingford CTWallingford CT, 2009.

26. T. Lu and F. Chen, *J. Comput. Chem*, 2012, **33**, 580-592.

27. G. García, M. Atilhan and S. Aparicio, *J. Mol. Liq*, 2015, **211**, 506-514.

28. H. J. C. Berendsen, D. van der Spoel and R. van Drunen, *Comput. Phys. Commun*, 1995, **91**, 43-56.

29. W.L. Jorgensen, and J. Tirado-Rives, *J. Am. Chem. Soc*, 1988, 110, 1657-1666.

30. L. Zhao, L. Liu and H. Sun, *J. Phys. Chem. C*, 2007, **111**, 10610-10617.

31. G. B. Arfken, and H. J. Weber, 1995, 1029.

32. G. Bussi, D. Donadio and M. Parrinello, *J. Chem. Phys*, 2007, **126**, 014101.

33. M. Parrinello and A. Rahman, *J. Appl. Phys*, 1981, **52**, 7182-7190.

34. W. F. Van Gunsteren and H. J. C. Berendsen, *Mol. Simul*, 1988, **1**, 173-185.

35. P. J. Hay and W. R. Wadt, *J. Chem. Phys*, 1985, **82**, 270-283.

36. M. Dolg, U. Wedig, H. Stoll and H. Preuss, *J. Chem. Phys*, 1987, **86**, 866-872.

37. V. Polo, J. Andres, S. Berski, L. R. Domingo and B. Silvi, *J. Phys. Chem. A*, 2008, **112**, 7128-7136.

38. A. S. C. Urcezino, L. P. M. Dos Santos, P. N. S. Casciano, A. N. Correia and P. De Lima-Neto, *J. Braz. Chem. Soc.*, 2017, **28**, 1193-1203.

39. D. Yue, Y. Jia, Y. Yao, J. Sun and Y. Jing, *Electrochim. Acta*, 2012, **65**, 30–36.

40. L. Vieira, R. Schennach and B. Gollas, *Electrochim. Acta*, 2016, **197**, 344-352.

41. E. I. Rogers, D. S. Silvester, D. L. Poole, L. Aldous, C. Hardacre and R. G. Compton, *J. Phys. Chem. C*, 2008, **112**, 2729-2735.

42. X.-J. Huang, E. I. Rogers, C. Hardacre and R. G. Compton, *J. Phys. Chem. B*, 2009, **113**, 8953-8959.

43. R. D. Shannon, *Acta Crystallogr. Sect. A*, 1976, **32**, 751-767.

44. M.V. Vener, A.V. Manaev, A.N. Egora, V.G. Tsirelson, *J. Phys. Chem. A*, 2007, **6**, 1155. D. Hugas, S.Simon, M. Duran, *Structural Chemistry*, 2005, **16**, 257. B.G. Oliveira, M.L.A.A. Vasconcellos, *J. Mol. Struct (THEOCHEM)*, 2007, **774**, 83. B.G. Oliveira, *J. Chil. Chem. Soc*, 2009, **54**, 43. B.G. Oliveira, M.L.A.A. Vasconcellos, *Acta Chim. Slov*, 2009, **56**, 340.

45. S. M. Soliman and A. Barakat, *Molecules*, 2016, **21**, 1669-1691.

Supplementary Material

Table S1. Effect of temperature on the viscosity of 1ChCl:2EG, 1ChCl:2U, and 1ChCl:2G containing 0.1 mol L^{-1} $CoCl_2.6H_2O$.

System	Temperature / K	η / mPa s[a]	a / nm
1ChCl:2EG	298	40.1	0.95
	312	23.0	
	333	12.6	
	353	7.75	
1ChCl:2U	298	574.4	1.06
	312	176.7	
	333	56.1	
	353	24.6	
1ChCl:2G	298	265.4	0.70
	312	113.4	
	333	46.0	
	353	22.8	

[a]1 Pa s = 10 g cm^{-1} s^{-1}

Table S2. The values of diffusion coefficients for Co^{2+} species calculated by the Cottrell method.

System	D / $cm^2\ s^{-1} \times 10^{-7}$	Temperature / K
$CoCl_2$ in 1ChCl:2EG	1.95 ± 0.54	298
$CoCl_2$ in 1ChCl:2EG	2.24 ± 0.07	313
$CoCl_2$ in 1ChCl:2EG	3.87 ± 0.07	333
$CoCl_2$ in 1ChCl:2EG	4.75 ± 0.50	353
$CoCl_2$ in 1ChCl:2U	0.18 ± 0.04	298
$CoCl_2$ in 1ChCl:2U	0.49 ± 0.05	313
$CoCl_2$ in 1ChCl:2U	0.72 ± 0.06	333
$CoCl_2$ in 1ChCl:2U	1.23 ± 0.22	353
$CoCl_2$ in 1ChCl:2G	0.13 ± 0.03	298
$CoCl_2$ in 1ChCl:2G	0.18 ± 0.09	313
$CoCl_2$ in 1ChCl:2G	1.36 ± 0.06	333
$CoCl_2$ in 1ChCl:2G	1.53 ± 0.22	353

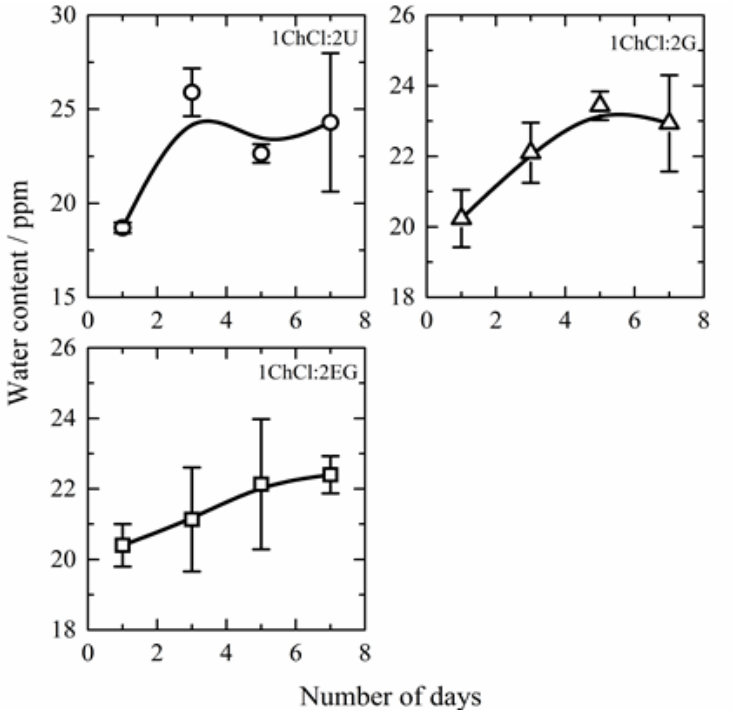

Fig. S1. The amount of water in DES in ppm as a function of the number of days under the ambient atmosphere. The results are an average of three measurements over a week.

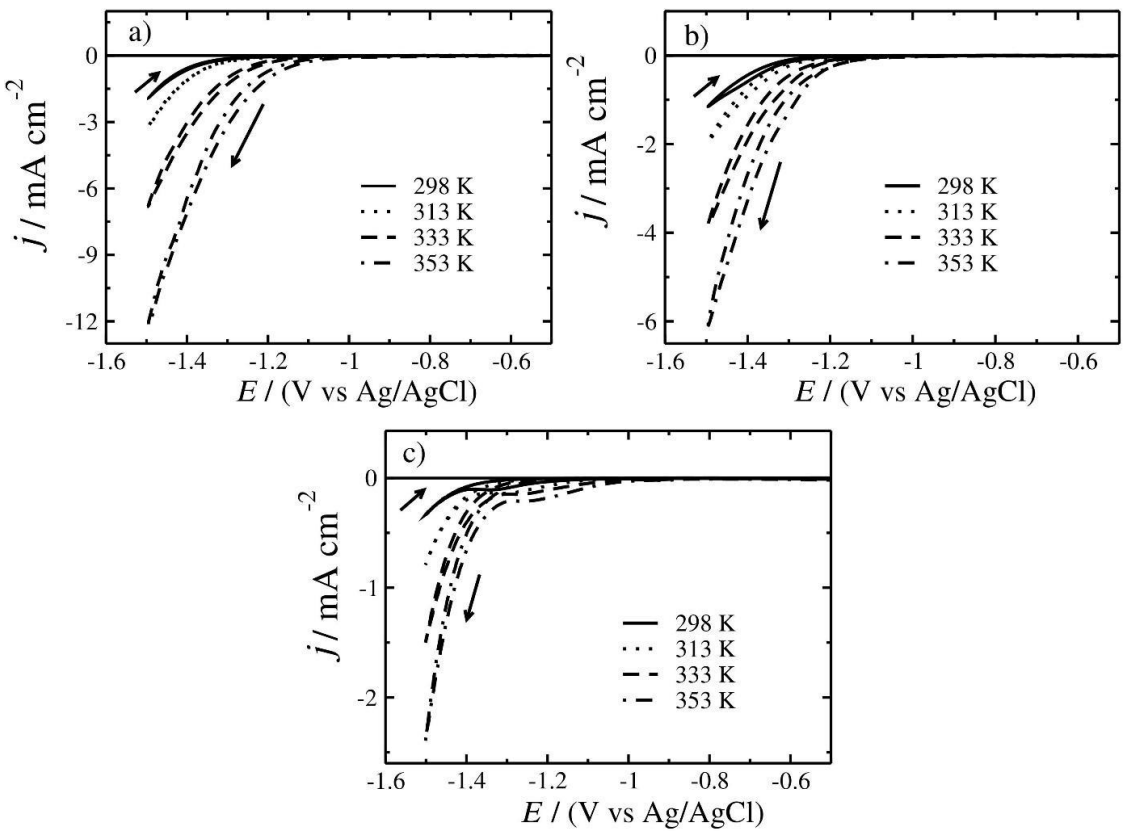

Fig S2. Cyclic voltammograms obtained for Cu electrode in (a) 1ChCl:2EG, (b) 1ChCl:2G, and (c) 1ChCl:2U blank electrolyte. Scan rate 10 mV s^{-1}.

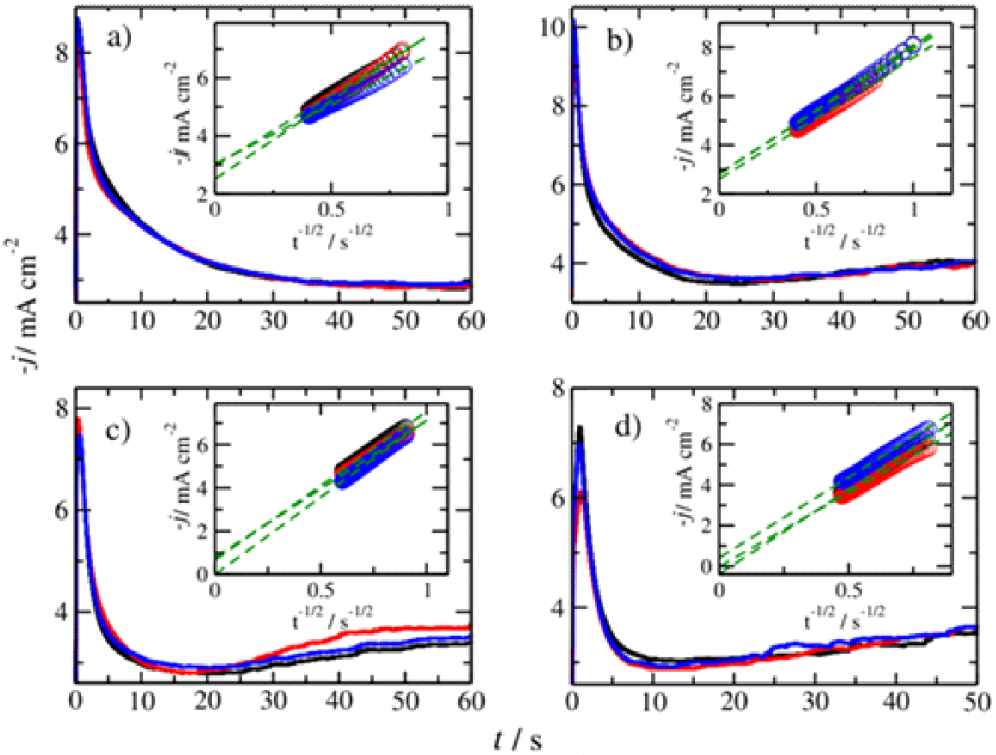

Fig S3. Current-time transients for the reduction of Co^{2+}/Co on Cu substrate obtained from DES 1ChCl:2EG (a) 298 K, (b) 313 K, (c) 333 K, and (d) 353 K containing 0.1 mol L^{-1} $CoCl_2.6H_2O$. Insets: Cottrell´s plots are showed as insert.

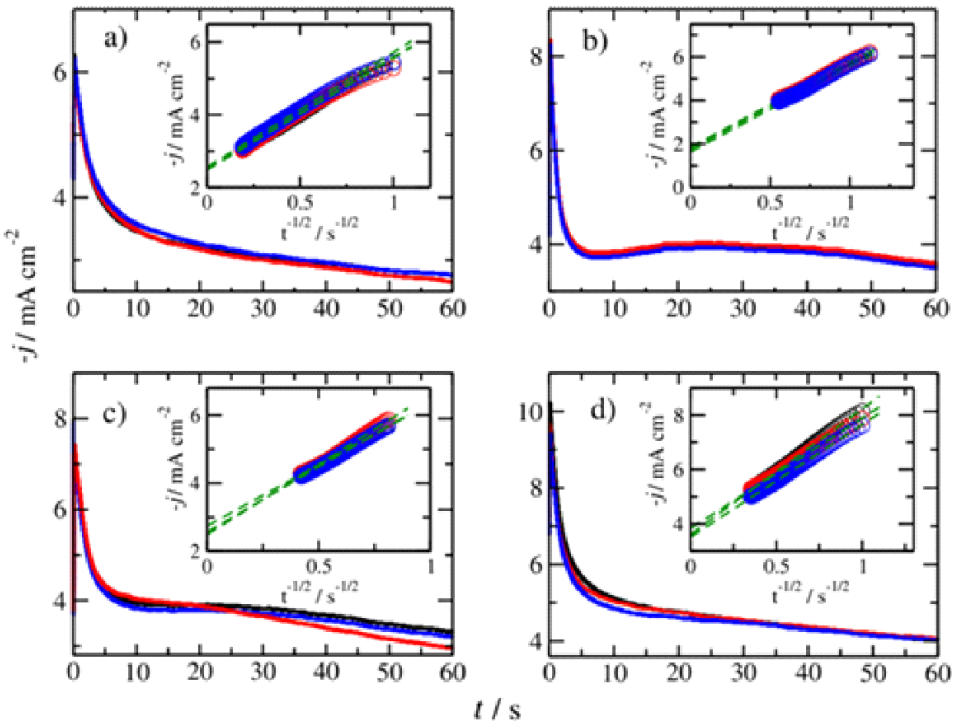

Fig. S4 Current-time transients for the reduction of Co^{2+}/Co on Cu substrate obtained from DES 1ChCl:2G (a) 298 K, (b) 313 K, (c) 333 K, and (d) 353 K containing 0.1 mol L^{-1} $CoCl_2.6H_2O$. Insets: Cottrell´s plots are showed as insert.

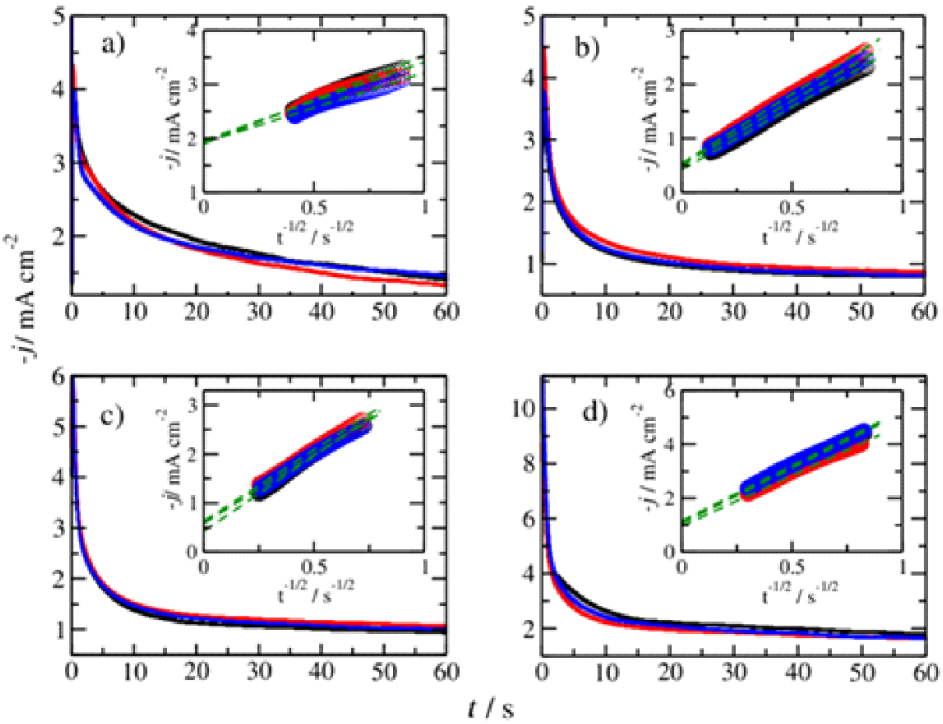

Fig. S5 Current-time transients for the reduction of Co^{2+}/Co on Cu substrate obtained from DES 1ChCl:2U (a) 298 K, (b) 313 K, (c) 333 K, and (d) 353 K containing 0.1 mol L^{-1} $CoCl_2.6H_2O$. Insets: Cottrell´s plots are showed as insert.

3 CONCLUSIONS

For all three electrolytes, the increase in the diffusion coefficient and decrease in the viscosity with increasing temperature was clearly apparent. The relationship could be quantified via the Cottrell and Arrhenius equations. Calculated values of the activation energies showed that energy barriers for the diffusion of Co^{2+} ions followed the following sequence: 1ChCl:2EG < 1ChCl:2U < 1ChCl:2G.

The simulations by molecular dynamics (MD) showed a strong interaction of anion chloride with Co^{2+} ions independent of temperature in the three systems analyzed. Besides, in the interval of temperature between 298 K and 353 K occurred the replaced of HBD molecules by anion chloride around Co^{2+} ions for SDW1 and SDW3 systems, while for SDW2 system this replaced occurred between 313 K and 353 K. The CN between Co^{2+} ions with water molecules did not showed changes significative with the increase temperature effect in the three systems analyzed. The simulations realized by QTAIM indicated that the Co-Cl interaction became stronger due to the increase of temperature in the three systems (SDW1, SDW2, and SDW3) analyzed. In contrast, the increase in temperature weakened the interaction between Co^{2+} ions with the oxygen of HBD molecules.

From a future perspective, we will analyze the behavior of Co^{2+} ions with the increase of percentage water in the three systems (SDW1, SDW2, and SDW3) studied, due that the RDF results in the three systems indicated a high probability of interaction between the Co^{2+} ions with oxygen water (Ow) molecules.

REFERENCES

ABBOTT, A. P. *et al*. A Comparative Study of Nickel Electrodeposition Using Deep Eutectic Solvents and Aqueous Solutions. **Electrochimica Acta**, *[s. l.]*, v. 176, p. 718–726, 2015.

ABBOTT, A. P. *et al*. Electrodeposition of copper composites from deep eutectic solvents based on choline chloride. **Physical Chemistry Chemical Physics**, *[s. l.]*, v. 11, n. 21, p. 4269–4277, 2009.

ABBOTT, A. P. *et al*. Electrodeposition of zinc-tin alloys from deep eutectic solvents based on choline chloride. **Journal of Electroanalytical Chemistry**, *[s. l.]*, v. 599, n. 2, p. 288–294, 2007.

ALCANFOR, A. A. C. *et al*. Electrodeposition of indium on copper from deep eutectic solvents based on choline chloride and ethylene glycol. **Electrochimica Acta**, *[s. l.]*, v. 235, p. 553–560, 2017.

BARRADO, E. et al. Electrodeposition of indium on W and Cu electrodes in the deep eutectic solvent choline chloride-ethylene glycol (1:2). **Journal of Electroanalytical Chemistry**, *[s. l.]*, v. 823, n. April, p. 106–120, 2018.

BEZERRA-NETO, João R.; BEZERRA, Lucas L.; SOUSA, Natalia G.; *et al*. Molecular approach about the effect of water on the electrochemical behaviour of Ag^{+} ions in urea-choline chloride-water mixture. **Journal of Molecular Modeling**, *[s. l.]*, v. 26, n. 12, p. 1–9, 2020.

BEZERRA-NETO, João R.; SOUSA, Natalia G.; DOS SANTOS, Luis P.M.; *et al*. The effect of water on the physicochemical properties of an ethylene glycol and choline chloride mixture containing Cu^{2+} ions: Electrochemical results and dynamic molecular simulation approach. **Physical Chemistry Chemical Physics**, *[s. l.]*, v. 20, n. 14, p. 9321–9327, 2018.

BEZERRA-NETO, João Rufino. **O efeito da água sobre as propriedades químicas dos íons Ag^{+} e Cu^{2+} em solventes eutéticos baseados em cloreto de colina.** 2018. 91 f. Tese (Doutorado em Química) – Pró-Reitoria de Pesquisa e Pós-Graduação, Universidade Federal do Ceará, Fortaleza, 2018.

CARRIAZO, Daniel; SERRANO, María Concepción; GUTIÉRREZ, María Concepción; *et al*. Deep-eutectic solvents playing multiple roles in the synthesis of polymers and related materials. **Chemical Society Reviews**, *[s. l.]*, v. 41, n. 14, p. 4996–5014, 2012.

GARCÍA, Gregorio; APARICIO, Santiago; ULLAH, Ruh; *et al*. Deep eutectic solvents: Physicochemical properties and gas separation applications. **Energy and Fuels**, *[s. l.]*, v. 29, n. 4, p. 2616–2644, 2015.

GORKE, Johnathan T.; SRIENC, Friedrich; KAZLAUSKAS, Romas J. Hydrolase-catalyzed biotransformations in deep eutectic solvents. **Chemical Communications**, *[s. l.]*, n. 10, p. 1235–1237, 2008.

LI, Y. *et al*. Construction of non-enzymatic sensor based on porous carbon matrix loaded with Pt and Co nanoparticles for real-time monitoring of cellular superoxide anions. **Electrochimica Acta**, *[s. l.]*, v. 294, p. 304–311, 2019.

LIM, J.; MAJETICH, S. A. Composite magnetic-plasmonic nanoparticles for biomedicine: Manipulation and imaging. **Nano Today**, *[s. l.]*, v. 8, n. 1, p. 98–113, 2013.

SARAVANAN, G.; MOHAN, S. Structure, composition and corrosion resistance studies of Co–Cr alloy electrodeposited from deep eutectic solvent (DES). **Journal of Alloys and Compounds**, *[s. l.]*, v. 522, p. 162–166, 2012

SEBASTIÁN, P.; VALLÉS, E.; GÓMEZ, E. Copper electrodeposition in a deep eutectic solvent. First stages analysis considering Cu(I) stabilization in chloride media. **Electrochimica Acta**, *[s. l.]*, v. 123, p. 285–295, 2014.

SMITH, Emma L.; ABBOTT, Andrew P.; RYDER, Karl S. Deep Eutectic Solvents (DESs) and Their Applications. **Chemical Reviews**, *[s. l.]*, v. 114, n. 21, p. 11060–11082, 2014.

SYED KHADAR, Y. A. *et al*. Synthesis, characterization and antibacterial activity of cobalt doped cerium oxide (CeO 2 :Co) nanoparticles by using hydrothermal method. **Journal of Materials Research and Technology**, *[s. l.]*, v. 8, n. 1, p. 267–274, 2019.

XU, C. *et al*. Facile in situ fabrication of Co nanoparticles embedded in 3D N-enriched mesoporous carbon foam electrocatalyst with enhanced activity and stability toward oxygen reduction reaction. **Journal of Materials Science**, *[s. l.]*, v. 54, n. 7, p. 5412–5423, 2019.

ZHANG, Qinghua; DE OLIVEIRA VIGIER, Karine; ROYER, Sébastien; *et al*. Deep eutectic solvents: Syntheses, properties and applications. **Chemical Society Reviews**, *[s. l.]*, v. 41, n. 21, p. 7108–7146, 2012.

ZHAO, Hua; BAKER, Gary A. Ionic liquids and deep eutectic solvents for biodiesel synthesis: A review. **Journal of Chemical Technology and Biotechnology**, *[s. l.]*, v. 88, n. 1, p. 3–12, 2013.

APPENDIX A – AUTOR'S CURRICULAR DATA

11/12/2021 Curriculum System of Curriculum Lattes (Lucas Lima Bezerra)

Lucas Lima Bezerra

Endereço para acessar este CV: http://lattes.cnpq.br/1266539768177026
ID Lattes: **1266539768177026**
Última atualização do currículo em 16/10/2021

Possui graduação em Química pela Universidade Estadual do Ceará (UECE). Atualmente, é mestrando em Química pelo Programa de Pós-Graduação em Química pela Universidade Federal do Ceará (UFC) e membro do Grupo de Química Teórica (GQT) - UFC. Experiência na área de Bioinformática e Química Computacional com ênfase nas simulações de solventes eutéticos, líquidos iônicos, biolubrificantes e receptor-ligante através das técnicas de Docking e Dinâmica Molecular. **(Texto informado pelo autor)**

Identificação

Nome	Lucas Lima Bezerra
Nome em citações bibliográficas	BEZERRA, L. L.
Lattes iD	http://lattes.cnpq.br/1266539768177026

Endereço

Formação acadêmica/titulação

2019	Mestrado em andamento em Química (Conceito CAPES 6). Universidade Federal do Ceará, UFC, Brasil. Título: Electrochemical and theoretical investigation on the behavior of the Co2+ ion in three eutectic solvents,Orientador: Norberto de Kássio Vieira Monteiro. Bolsista do(a): Coordenação de Aperfeiçoamento de Pessoal de Nível Superior, CAPES, Brasil.
2014 - 2018	Graduação em Química. Universidade Estadual do Ceará, UECE, Brasil. Título: Avaliação in silico do potencial farmacológico dos carotenoides presentes em Bixa Orellana contra o vírus da dengue. Orientador: Emmanuel Silva Marinho. Bolsista do(a): Fundação Cearense de Apoio ao Desenvolvimento Científico e Tecnológico, FUNCAP, Brasil.
2000 - 2013	Ensino Médio (2º grau). Colégio Lima Nogueira, CLN, Brasil.

Formação Complementar

2015	Inglês. (Carga horária: 360h). Núcleo de Línguas- Itaperi, NL, Brasil.
2021 - 2021	Dinâmica Molecular Básica. (Carga horária: 10h). Laboratório Nacional de Computação Científica, LNCC, Brasil.
2021 - 2021	Métodos Quânticos Semiempíricos: Teoria e Prática. (Carga horária: 10h). Laboratório Nacional de Computação Científica, LNCC, Brasil.
2020 - 2020	ESTUDOS COMPUTACIONAIS DE AGENTES TERAPÊUTICOS PARA A COVID-19. (Carga horária: 6h). Universidade Federal do Ceará, UFC, Brasil.
2020 - 2020	INTRODUÇÃO AO ORIGIN. (Carga horária: 6h). Universidade Federal do Ceará, UFC, Brasil.
2019 - 2019	Modelagem Molecular. (Carga horária: 6h). Universidade Federal do Ceará, UFC, Brasil.
2017 - 2017	Técnicas Avançadas e Estratégias de Isolamento de Produtos Naturais. (Carga horária: 7h). Universidade Estadual do Ceará, UECE, Brasil.
2016 - 2016	Ciência dos materiais. (Carga horária: 12h). Universidade Estadual do Ceará, UECE, Brasil.

2016 - 2016 Introdução a Química Computacional na Modelagem de Fármacos. (Carga horária: 12h). Universidade Estadual do Ceará, UECE, Brasil.

2012 - 2013 Hardware - Montagem e Manutenção. (Carga horária: 64h). Centro Brasileiro de Cursos, CEBRAC, Brasil.

Atuação Profissional

Colégio 7 de Setembro, C7S, Brasil.

Vínculo institucional

2018 - 2018 Vínculo: Bolsista, Enquadramento Funcional: Monitor das turmas do terceiro ano/ENEM, Carga horária: 20

Universidade Estadual do Ceará, UECE, Brasil.

Vínculo institucional

2017 - 2018 Vínculo: Bolsista, Enquadramento Funcional: IC/UECE, Carga horária: 20, Regime: Dedicação exclusiva.

Vínculo institucional

2016 - 2017 Vínculo: Bolsista, Enquadramento Funcional: ICT/FUNCAP, Carga horária: 20, Regime: Dedicação exclusiva.

Áreas de atuação

1. Grande área: Ciências Exatas e da Terra / Área: Química.

Idiomas

Inglês Compreende Bem, Fala Razoavelmente, Lê Bem, Escreve Bem.

Português Compreende Bem, Fala Bem, Lê Bem, Escreve Bem.

Prêmios e títulos

2017 Menção Honrosa na XXX Jornada Brasileira de Iniciação científica em Química, Congresso Brasileiro de Química.

Produções

Produção bibliográfica

Artigos completos publicados em periódicos

Ordenar por

Ordem Cronológica

1. BEZERRA-NETO, J. R. ; **BEZERRA, L. L.** ; SOUSA, G, N. ; SANTOS, L. P. M. ; MARINHO, E. S. ; MONTEIRO, N. K. V. ; CORREIA, A. N. ; LIMA-NETO, P. . Molecular approach about the effect of water on the electrochemical behaviour of Ag+ ions in urea-choline chloride-water mixture. JOURNAL OF MOLECULAR MODELING (ONLINE) JCR, v. 1, p. 1-8, 2020.
2. **BEZERRA, L. L.**; MARINHO, M. M. ; MARINHO, E. S. . Molecular Docking Studies Between Anthraquinone Aloe Emodin and Dengue VIrus Protein (Denv-2). International Journal of Recent Research and Review, v. XI, p. 14-18, 2018.
3. **BEZERRA, L. L.**; MARINHO, E. S. ; MARINHO, M. M. . Allicin an Inhibiting Potential of HIV Virus: A Molecular Docking Studies Comparative with the Ritonavir® Inhibitor. International Journal of Recent Research and Review, v. XI, p. www.ijrrr.com, 2018.
4. LIMA, A,R. ; SILVA, J. ; **BEZERRA, L. L.** ; MARINHO, M. M. ; MARINHO, E. S. . Molecular docking of potential curcuminoids inhibitors of the NS1 protein of dengue virus.. INTERNATIONAL JOURNAL OF SCIENTIFIC AND ENGINEERING RESEARCH, v. 8, p. 861-868, 2017.
5. SILVA, J. ; LIMA, A,R. ; **BEZERRA, L. L.** ; MARINHO, M. M. ; MARINHO, E. S. . Bixinoids potentially active against dengue virus: a molecular docking study.. INTERNATIONAL JOURNAL OF SCIENTIFIC AND ENGINEERING RESEARCH, v. 8, p. 882-887, 2017.

6. SILVA, J. ; LIMA, A,R. ; **BEZERRA, L. L.** ; MARINHO, M. M. ; MARINHO, E. S. . Molecular coupling study between the potential inhibitor of dengue fever, Annatto and Protein E (DENV-4). INTERNATIONAL JOURNAL OF SCIENTIFIC AND ENGINEERING RESEARCH, v. 8, p. 815-821, 2017.

7. **BEZERRA, L. L.**; SILVA, J. ; LIMA, A,R. ; MARINHO, M. M. ; MARINHO, E. S. . Docking molecular studies between the bixin and norbxin carotenoids and the Dengue Fever Virus (NS1). INTERNATIONAL JOURNAL OF SCIENTIFIC AND ENGINEERING RESEARCH, v. 8, p. 520-526, 2017.

Trabalhos completos publicados em anais de congressos

1. **BEZERRA, L. L.**; MARINHO, M. M. . Aloe emodin: um potencial inibidor do vírus da dengue. In: XXIII Encontro de iniciação a pesquisa, 2017, Fortaleza. XXIII Encontro de Iniciação a Pesquisa, 2017.
2. **BEZERRA, L. L.**; MARINHO, E. S. . Caracterização eletrônico/estrutural do fármaco anti-hipertensivo Alprenolol: um estudo quântico semi-empírico. In: XXIII Encontro de Iniciação a Pesquisa, 2017, Fortaleza. XXIII Encontro de Iniciação a Pesquisa, 2017.
3. **BEZERRA, L. L.**; MARINHO, M. M. ; MARINHO, E. S. . Utilização da teoria do funcional da densidade(DFT) para caracterização estrutural do fármaco Gaboxadol: MESP, HOMO e LUMO. In: XXI Semana Universitária da UECE, 2016, Fortaleza. XXI Semana Universitária da UECE, 2016.

Resumos expandidos publicados em anais de congressos

1. **BEZERRA, L. L.**; MARINHO, M. M. ; MARINHO, E. S. . Estudo eletrônico/estrutural do fármaco sintético Tavaborole: Uma abordagem quântica semi-empírica. In: 57º Congresso Brasileiro de Química, 2017, Gramado. 57º Congresso Brasileiro de Química, 2017.
2. **BEZERRA, L. L.**; MARINHO, M. M. ; MARINHO, E. S. . Caracterização da interação entre a antraquinona presente no Aloe vera, barbaloína e a proteína SN1, presente no vírus da dengue tipo-I. In: 57º Congresso Brasileiro de Química, 2017, Gramado. 57º Congresso Brasileiro de Química, 2017.
3. **BEZERRA, L. L.**; MARINHO, M. M. ; MARINHO, E. S. . ESTUDOS PRELIMINARES DE MODELAGEM MOLECULAR DO FÁRMACO SINTÉTICO MACITENTAN. In: XXII - ENCONTRO DE INICIAÇÃO À PESQUISA DA UNIFOR, 2016, Fortaleza. Anais do XII Encontro de Iniciação à Pesquisa da Unifor, 2016.

Resumos publicados em anais de congressos

1. OLIVEIRA, A. P. S ; LIMA, D. R. ; **BEZERRA, L. L.** ; MONTEIRO, N. K. V. ; PESSOA, O. D. L ; SILVA, M. G. V . In silico study of flavonoids from the genus Chamaecrista: ADME, pharmacokinetic properties and molecular dynamics. In: Brazilian Conference on Natural Products, 2021, Espirito Santo. Brazilian Conference on Natural Products, 2021.
2. **BEZERRA, L. L.**; SILVA, J. ; LIMA, A,R. ; SILVA, L,P. ; MARINHO, M. M. ; MARINHO, E. S. . Caracterização inicial do fármaco antifúngico tavaborole para estudos de modificação molecular (drug design). In: XXII Semana Universitária da Uece, 2017, Fortaleza. XXII Semana Universitária da Uece, 2017.
3. **BEZERRA, L. L.**; SILVA, J. ; LIMA, A,R. ; SILVA, L,P. ; MARINHO, M. M. ; MARINHO, E. S. . Estudos iniciais de modificação molecular (drug design) do fármaco anti-hipertensivo Alprenolol. In: XXII Semana Universitária da Uece, 2017, Fortaleza. XXII Semana Universitária da Uece, 2017.
4. SOUZA, B,D. ; LIMA, A,R. ; SILVA, J. ; **BEZERRA, L. L.** ; FILHO, L,C,M ; MARINHO, M. M. ; MARINHO, E. S. . Caracterização estrutural do fármaco anagliptin: Um estudo in silico. In: Semana Universitária da UECE, 2017, Fortaleza. Semana Universitária da UECE, 2017.
5. BARBOSA, K,L. ; MARINHO, E. S. ; **BEZERRA, L. L.** ; SILVA, J. ; LIMA, A,R. ; CARNEIRO, S,S. ; MARINHO, M. M. . Caracterizaçao Eletronica do Farmaco Difunisal: Aplicaçao do Campo de Força Classico MMFF94 para Identificaçao dos Sitios Reacionais. In: XXII Semana Universitaria da UECE, 2017, Fortaleza. XXII Semana Universitaria da UECE, 2017.
6. **BEZERRA, L. L.**; MARINHO, M. M. ; MARINHO, E. S. . Estudo in silico preliminar de modelagem molecular do fármaco gaboxadol. In: XXI Semana Universitária da UECE, 2016, Fortaleza. XXI Semana Universitária da UECE, 2016.

Eventos

Participação em eventos, congressos, exposições e feiras

1. X Escola de Modelagem Molecular em Sistemas Biológicos.X Escola de Modelagem Molecular em Sistemas Biológicos. 2021. (Simpósio).
2. X Semana da Química da UFC e III Workshop da Pós-Graduação em Química.Modelagem Molecular. 2019. (Outra).
3. 57° Congresso Brasileiro de Química. 57° Congresso Brasileiro de Química. 2017. (Congresso).
4. III Ciclo de Palestras da Química.III Ciclo de Palestras da Química. 2017. (Encontro).
5. II Ciclo de Palestras da Química.II Ciclo de Palestras da Química. 2016. (Outra).
6. III Feira das profissões da Universidade Estadual do Ceará. III Feira das profissões da Universidade Estadual do Ceará. 2016. (Feira).
7. I Ciclo de Palestras da Química.I Ciclo de Palestras da Química. 2015. (Outra).

APPENDIX B – PAPER PUBLISHED

Journal of Molecular Modeling (2020) 26:339
https://doi.org/10.1007/s00894-020-04587-y

ORIGINAL PAPER

Molecular approach about the effect of water on the electrochemical behaviour of Ag^+ ions in urea-choline chloride-water mixture

João R. Bezerra-Neto[1] · Lucas L. Bezerra[1] · Natalia G. Sousa[1] · Luis P. M. dos Santos[1] · Emmanuel S. Marinho[2] · Norberto K. V. Monteiro[1] · Adriana N. Correia[1] · Pedro de Lima-Neto[1]

Received: 27 March 2020 / Accepted: 25 October 2020

Abstract
The water influence on electrochemical behaviour of Ag^+ ions in urea and choline chloride mixture was investigated by cyclic voltammetry technique, while the molecular insights about the investigated systems were obtained from molecular dynamic (MD) simulation. The water content was variated from 0 up to 10% (v/v). Cyclic voltammetry technique showed that the peak potential for Ag^+/Ag redox couples shifted in direction to more positive potentials with the gradual increase of water content in solution, indicating that the addition of water electrocatalyses the kinetics of the reduction of Ag^+ ions. The MD simulations demonstrated that water molecules do not interact strongly with Ag^+ ions but induce a small reduction in the number of urea molecules around of the ion and that the water molecules adjust to free spaces in the mixture.

Keywords Deep eutectic solvents · Reline · Molecular dynamic · Cyclic voltammetry · Ag^+ ions

Introduction

Silver electrodeposited coating has high corrosion resistance; it presents good electric conductivity and it is bright [1, 2]. These properties allow its use as cover coating in electronic devices to protect the metals against corrosion and, furthermore, it improves the final appearance of the industrial product. In electroplating industries, silver coating is traditionally obtained from aqueous plating solution containing cyanide as complexing agent, which is one of the top toxic chemicals. The necessity of this chemical, or other non-environmentally friendly chemicals, is the main disadvantage related to the silver industrial plating process since a non-environmental safety industrial wastewater need to be discharged [3].

Therefore, it is relevant to investigate alternative electroplating formulations that come to allow the silver electrodeposition, and the electrodeposition of others noble metals, from plating solutions formulated with environmentally friendly chemicals. In this direction, it is increasing the use of the named deep eutectic solvents (DESs) to electrodeposit metal and alloys, since they have interesting chemical and physical properties, such as good ionic conductivity, high thermal stability, the metal salts are soluble in them, they are non-toxic and biodegradable, their production is of low cost and, finally, they present electrochemical stability in a large potential range [4–7]. These mixtures are prepared mixing a quaternary ammonium halide salt with a hydrogen-bond donor (HBD) molecule.

Due to the importance of this metal and the advantages offered by the eutectic solvents, the silver electrodeposition in DESs has been studied. Abbott et al. [8] described that the wear resistance of silver coatings can be achieved from the electrolytic deposition of silver from a solution of AgCl in an ethylene glycol/choline chloride mixture. The electrodeposition of silver in a eutectic mixture of 1 choline chloride:2 urea

APPENDIX C – PAPER SUBMITTED

Journal of Molecular Graphics and Modelling

Electrochemical and theoretical investigation on the behavior of the Co2+ ion in three eutectic solvents

--Manuscript Draft--

Manuscript Number:	JMGM-D-21-00978
Article Type:	Full Length Article
Keywords:	Deep eutectic solvents; Cobalt; Electrochemical techniques; Computational simulations
Corresponding Author:	Norberto Monteiro Universidade Federal do Ceara BRAZIL
First Author:	Lucas Lima Bezerra
Order of Authors:	Lucas Lima Bezerra
	Francisco Gilvane Sampaio Oliveira
	Luis Paulo Mourão dos Santos
	Hosiberto Batista de Sant'Ana
	Filipe Xavier Feitosa
	Adriana Nunes Correia
	Walther Schwarzacher
	Emmanuel Silva Marinho
	Pedro de Lima-Neto
	Norberto Monteiro
Abstract:	Deep eutectic solvents (DESs) have many advantages, making them a promising alternative in replacing ionic liquids and organic solvents. Besides, DESs has received much prominence due to its diverse applications: Electrodeposition of metals, organic synthesis, gas adsorption, and biodiesel production. Therefore, this work analyzed the effect of the temperature increase (298 K to 353 K) on the behavior of the Co^{2+} ions in three eutectic solvents through electrochemical techniques and computational simulations. From the electrochemical analysis carried out, the increase in temperature caused a reduction in specific mass and an increase in the diffusion coefficient. Besides, the activation energy values were of 15.3, 29.9, and 55.2 kJ mol^{-1} for 1ChCl:2EG, 1ChCl:2U, and 1ChCl:2G, respectively. The computational simulations indicate that the increased temperature effect caused the replacement of HBD molecules by anions chloride around Co^{2+} ions for the SDW1 and SDW3 systems between the temperatures of 298 K to 353 K, except for the SDW2 system that the replaced occurred in the interval of 313 K to 353 K. Besides, the increase of temperature occasioned the increase of strength for Co-Cl interaction and weakened the interactions between the Co^{2+} ions with the oxygen of HBD molecules.

Physical Chemistry Chemical Physics

PCCP

Sulfonamide derived from anacardic acid as potential anti-sores: a theoretical approach based on Molecular Docking, Molecular Dynamics, and Density Functional Theory calculations

Journal:	*Physical Chemistry Chemical Physics*
Manuscript ID	CP-ART-08-2021-003995.R1
Article Type:	Paper
Date Submitted by the Author:	n/a
Complete List of Authors:	da Silva, Leonardo; Universidade Federal do Ceará, Química Analítica e Físico-Química Wagner Queiroz Neto, Francisco; Universidade Federal do Ceará, Analítica e Físico Química Bezerra, Lucas; Universidade Federal do Ceara, Química Analítica e Físico-Química Silva, Jacilene; Universidade Regional do Cariri Monteiro, Norberto; Federal University of Ceará Technology Centre, Marinho, Marcia; Universidade Federal do Ceará, Departamento de Farmácia; dos Santos, Helcio; Universidade Estadual Vale do Acaraú Teixeira, Alexandre; Universidade Regional do Cariri Marinho, Emmanuel; Universidade Estadual do Ceará Lima-Neto, Pedro; Universidade Federal do Ceara, Quimica Analitica e Físico-Quimica

JAOCS
JOURNAL OF THE AMERICAN OIL CHEMISTS' SOCIETY

Green lubricants production from Nile tilapia waste and prediction of physical properties through molecular dynamics simulations

Journal:	*Journal of the American Oil Chemists' Society*
Manuscript ID	JAOCS-21-0305
Manuscript Type:	Original Article
Date Submitted by the Author:	28-Nov-2021
Complete List of Authors:	Ramos Moreira, Denise; Department of Organic and Inorganic Chemistry Nery Ferreira, Elano ; Federal University of Ceara, Department of Organic and Inorganic Chemistry Câmara Neto, João Francisco; Federal University of Ceara, Department of Organic and Inorganic Chemistry Lima Bezerra, Lucas ; Federal University of Ceara, Department of Physical Chemistry and Analytical Chemistry Vieira Monteiro, Norberto de Kássio ; Federal University of Ceara, Department of Physical Chemistry and Analytical Chemistry Peixoto do Valle , Camila ; Federal University of Ceara, Department of Organic and Inorganic Chemistry Bezerra Mota Gomes Arruda, Tathilene ; Federal University of Ceara, Department of Organic and Inorganic Chemistry Lima Neto, Pedro; Federal University of Ceara, Department of Physical Chemistry and Analytical Chemistry Silva Rodrigues , Jailson ; Federal University of Ceara, Department of Organic and Inorganic Chemistry Arruda Rodrigues , Francisco Eduardo ; Federal Institute of Education Science and Technology of Ceara Petzhold, Cesar; Federal University of Rio Grande do Sul, Chemical Institute Maier, Martin; Eberhard Karls Universität Tübingen, Institut für Organische Chemie Ricardo, Nágila Maria; Federal University of Ceara, Chemistry
Keywords:	Lubricants < Biobased Products, Co-products (Waste) < Biobased Products, Fats and oils, Oxidative Stability < Food and Feed Science / Nutrition and Health, Esterification < Processing Technology, Rheology < Lipid Chemistry / Lipid Analysis

Journal of Molecular Liquids

Analysis of the behavior of Sn2+ and In3+ ions in DES and in water: a theoretical approach

--Manuscript Draft--

Manuscript Number:	MOLLIQ-D-21-07005
Article Type:	Full length article
Section/Category:	Ionic liquids
Keywords:	DES; Water; Tin; Indium; MD; QTAIM
Corresponding Author:	Norberto Monteiro Federal University of Ceará Fortaleza, Brazil
First Author:	Renato Veríssimo de Oliveira
Order of Authors:	Renato Veríssimo de Oliveira
	Lucas Lima Bezerra
	Natália Gomes Sousa
	Filipe Feitosa
	Hosilberto Batista de Sant'Ana
	Adriana Nunes Correia
	Pedro de Lima-Neto
	Norberto Monteiro
Abstract:	In an attempt to replace conventional organic solvents and ionic liquids, the Deep Eutectic Solvents (DES) emerged, the class of compounds with essential properties in the industry. These solvents have numerous advantages regarding ionic liquids, such as low price, biodegradability, and low toxicity. Furthermore, the DES has many applications in science, for example, organic synthesis, electrodeposition of metals, catalytic process. In this work, Sn 2+ and In 3+ ions behavior was analyzed in the solvents 1ChCl:2EG (chloride choline and ethylene glycol, DES) and water through computational simulations by molecular dynamics (MD) and quantum calculations of QTAIM. The results showed that the Sn 2+ and In 3+ ions strongly interact with the chloride anion in DES. In contrast, the most likely interaction is between cations and oxygen from water in a water solvent. The analysis of critical binding points (BCPs) showed that the strength of these interactions follows the following sequence: Sn-Ow > Sn-Cl and In-Ow > In-Cl. The behavior of both ions in the metallic mixture was invariant in DES when compared to the same isolated ions. However, for the aqueous system,

Journal of the Brazilian Chemical Society

Flavonoids from *Chamaecrista* genus: virtual screening, ADME and pharmacokinetic properties, interactions of flavonoid-DNA complex by molecular docking and molecular dynamics

Journal:	*Journal of the Brazilian Chemical Society*
Manuscript ID	JBCHS-2021-0398
Manuscript Type:	Article
Date Submitted by the Author:	28-Oct-2021
Complete List of Authors:	Oliveira, Ana Paula ; Universidade Federal do Ceará, Department of Organic and Inorganic Chemistry Lima, Daniele ; Federal University of Ceará, Departament of Organic and Inorganic Chemistry Bezerra, Lucas ; Federal University of Ceará, Department of Physico-chemical and Analytical chemistry Monteiro, Norberto ; Universidade Federal do Ceara Centro de Ciencias Loilola, Otília; Federal University of Ceará, Departament of Organic and Inorganic Chemistry Silva, Maria Goretti; Federal University of Ceará, Departament of Organic and Inorganic Chemistry; Federal University of Ceará, Department of Physico-chemical and Analytical chemistry
Keyword:	drug-like inhibitors, tumoral DNA, Molecular Dynamics, Chamaecrista, in silico
Please, specify if the submission is for a Regular Issue or Special Issue:	Regular Issue

SPRINGER NATURE SNAPP

Your submissions

Track your submissions

Insulin receptor-binding multifunctional protein from Tamarindus indica L. and presents hypoglycemic effect in a diet-induced type 2 diabetes preclinical study

Corresponding Author: Ana Heloneida Araújo Morais

Scientific Reports

bbfef7fc-ed77-4ea9-b0b2-c4ae7dbf7aa7 | v.1.0

Quality check in progress

about 7 hours ago